Zermelo navigation on the sphere with revolution metrics

Bernard Bonnard* Olivier Cots† Yannick Privat‡§ Emmanuel Trélat¶

February 1, 2024

Abstract

In this article motivated by physical applications, the Zermelo navigation problem on the two-dimensional sphere with a revolution metric is analyzed within the framework of minimal time optimal control. The Pontryagin maximum principle is used to compute extremal curves and a neat geometric frame is introduced using the Carathéodory-Zermelo-Goh transformation. Assuming that the current is of revolution, the geodesics are sorted according to a Morse-Reeb classification. We then illustrate the relevance of this classification using various examples from physics: the Lindblad equation in quantum control, the averaged Kepler case in space mechanics and the Landau-Lifshitz equation in ferromagnetism.

Keywords: Zermelo navigation problem; Minimal time geometric control; Morse-Reeb classification.

1 Introduction

A Zermelo navigation problem on the two-dimensional sphere M with a revolution metric is defined by a pair (g, F_0) where g is a metric of revolution on M and F_0 is a smooth vector field on M called the *current*. Using the control framework [9], the problem can be formulated as a *minimal time transfer problem* between two points $q_0, q_1 \in M$ for the single-input control-affine system

$$\frac{\mathrm{d}q}{\mathrm{d}t}(t) = F_0(q(t)) + \sum_{i=1}^{2} u_i(t)\, F_i(q(t)), \tag{1}$$

where the control $u = (u_1, u_2)$ is subject to the constraint $\|u\|^2 = u_1^2 + u_2^2 \leqslant 1$ and $q = (r, \theta)$ are the polar coordinates for the metric of revolution $g = \mathrm{d}r^2 + m^2(r)\,\mathrm{d}\theta^2$ with $m(r) > 0$ (see [2]). The two smooth vector fields

$$F_1 = \frac{\partial}{\partial r}, \quad F_2 = \frac{1}{m(r)}\frac{\partial}{\partial \theta}$$

form an orthonormal frame, and the current F_0 is

$$F_0(q) = \mu_1(q)\frac{\partial}{\partial r} + \mu_2(q)\frac{\partial}{\partial \theta}$$

*Institut Mathématique de Bourgogne and INRIA Sophia Antipolis (bernard.bonnard@u-bourgogne.fr).

†Institut de Recherche en Informatique de Toulouse, UMR CNRS 5505, Université de Toulouse, INP-ENSEEIHT, France (olivier.cots@irit.fr).

‡Université de Lorraine, CNRS, Institut Elie Cartan de Lorraine, Inria, BP 70239 54506 Vandœuvre-lès-Nancy Cedex, France. (yannick.privat@univ-lorraine.fr).

§Institut Universitaire de France (IUF)

¶Sorbonne Université, CNRS, Université Paris Cité, Inria, Laboratoire Jacques-Louis Lions (LJLL), F-75005 Paris, France (emmanuel.trelat@sorbonne-universite.fr).

where $\mu_1(q)$ is the *vertical* component and $\mu_2(q)$ is the *horizontal* component. The current is said to be of revolution if μ_1 and μ_2 do not depend on θ. The surface M is the (closure of) the union of two domains: the region of weak current where $\|F_0\|_g < 1$ and the region of strong current where $\|F_0\|_g > 1$.

The above problem is a generalization of the historical problem of the *quickest nautical path* introduced and studied by Carathéodory and Zermelo in [10, 21] where one can find a complete study in the case of a linear current, the metric being the Euclidean metric.

Borrowing the point of view of the historical problem, a neat geometric frame was introduced in [21], parametrizing the curves by the *heading angle* α of the ship, extending the control system to a single-input control-affine system

$$\frac{\mathrm{d}\tilde{q}}{\mathrm{d}t}(t) = X(\tilde{q}(t)) + v(t)\, Y(\tilde{q}(t))$$

where $\tilde{q} = (r, \theta, \alpha)$ and v is the time derivative of α. This transform, referred to as the *Carathéodory-Zermelo-Goh* transformation, leads to analyze the problem using iterated *Lie brackets* of the vector fields X and Y.

In this article we perform the analysis in the case of revolution. Thanks to *Clairaut condition*, the extremal dynamics can be integrated and studied using an extension of the *Morse-Reeb classification* for 2D Hamiltonian system [3]. Preliminary results where obtained in [5] in the case of an horizontal current and are here extended to the general case. Extremal curves are sorted by distinguishing r-periodic and r-aperiodic curves.

Another contribution of this article is to analyze three case studies. The first is the so-called *averaged Kepler case*, appearing also in space mechanics [3]. Geometrically it amounts to analyzing the effect of the curvature on the historical example. It is a case of revolution, with horizontal current only. The second case comes from quantum control and is related to the control of the Lindblad equation. We propose a simplified dynamics model corresponding to a case of revolution with vertical current. The final study, based on [11], concerns the Landau-Lifshitz model for ellipsoidal ferromagnetic samples. We propose an alternative frame to study the controllability problem of the magnetic moment.

The article is organized in two sections. In Section 2, we recall the Pontryagin maximum principle [16] and we present the geometric tools to analyze the extremals. The Carathéodory-Zermelo-Goh transformation is introduced in details to classify the extremals with respect to the induced action of the feedback group. In the case of revolution, the Morse-Reeb classification is introduced to refine the classification of the extremals. It amounts roughly to extending the Liouville-Mineur-Arnold theorem [2]. Extremals are either r-periodic or r-aperiodic curves, in relationship with weak and strong current domains. Section 3 provides the details of the analysis in three case studies.

2 Pontryagin maximum principle and geometric analysis of the Hamiltonian dynamics

2.1 Pontryagin maximum principle

For $i \in \{1, 2\}$, let F_i be a smooth vector field on M; we denote by $H_i(q, p) = \langle p, F_i(q) \rangle$ the Hamiltonian lift, in local coordinates $z = (q, p)$ the coordinates on T^*M with $p = (p_r, p_\theta)$ (adjoint vector). The *pseudo-Hamiltonian* is the cost-extended Hamiltonian defined by

$$H(z, u) = H_0(z) + \sum_{i=1}^{2} u_i\, H_i(z) + p^0$$

where $p^0 \in \mathbb{R}$ is the dual variable of the cost. We define the maximized Hamiltonian by

$$M(z) = \max_{\|u\| \leq 1} H(z, u).$$

According to the Pontryagin maximum principle [16], any minimal (or maximal) time trajectory, solution of (1) on $[0\,, t_f]$, must be the projection onto M of an extremal, that is a quadruple $(q(\cdot), p(\cdot), p^0, u(\cdot))$, with $(p(\cdot), p^0) \neq (0, 0)$, satisfying

$$\frac{\mathrm{d}q}{\mathrm{d}t}(t) = \frac{\partial H}{\partial p}(z(t), u(t)), \quad \frac{\mathrm{d}p}{\mathrm{d}t}(t) = -\frac{\partial H}{\partial q}(z(t), u(t)), \tag{2}$$

and the maximization condition

$$H(z(t), u(t)) = M(z(t)) \tag{3}$$

for almost every $t \in [0\,, t_f]$. Moreover, we have $M(z(t)) = 0$ for every $t \in [0\,, t_f]$. Furthermore, if the trajectory is minimal time then $p^0 \leq 0$ and if the trajectory is maximal time then $p^0 \geq 0$.

The projection onto M of an extremal is called a *geodesic*. Then, the Pontryagin maximum principle says that any minimal time trajectory must be a geodesic. Recall anyway that this is only a necessary condition for optimality and that, conversely, a geodesic may fail to be minimal time. A geodesic is said to be *strict* if it has a unique extremal lift, up to scaling. An extremal is said to be *normal* if if $p^0 \neq 0$ and *abnormal* (or exceptional) if $p^0 = 0$. In the normal case, it is said to be *hyperbolic* if $p^0 < 0$ and *elliptic* if $p^0 > 0$.

In the present situation, it follows from the maximization condition that:

- extremal controls are given by $u_i(z) = H_i(z)/\|p\|_g$, for $i = 1, 2$, where

$$\|p\|_g = \big(H_1^2(z) + H_2^2(z)\big)^{1/2} = \left(p_r^2 + \frac{p_\theta^2}{m^2(r)}\right)^{1/2};$$

- the maximized Hamiltonian is $M(z) = H_0(z) + \|p\|_g + p^0$;

- any extremal is solution of the Hamiltonian system

$$\frac{\mathrm{d}q}{\mathrm{d}t}(t) = \frac{\partial M}{\partial p}(z(t)), \qquad \frac{\mathrm{d}p}{\mathrm{d}t}(t) = -\frac{\partial M}{\partial q}(z(t)).$$

2.2 Carathéodory-Zermelo-Goh transformation and geodesics parameterization

In their seminal study, Carathéodory and Zermelo introduced the heading angle to parameterize the geodesics [10], which amounts to using the Goh transformation in optimal control. Since for the geodesics one has $\|u\| = 1$, one can set $u = (\cos\alpha, \sin\alpha)$, α being the heading angle of the ship. Let $\tilde{q} = (q, \alpha)$ be the extended state and set

$$X(\tilde{q}) = F_0(q) + \cos\alpha\, F_1(q) + \sin\alpha\, F_2(q), \quad Y(\tilde{q}) = \frac{\partial}{\partial\alpha}.$$

This leads to augment (1) to the single-input control-affine system:

$$\frac{\mathrm{d}\tilde{q}}{\mathrm{d}t}(t) = X(\tilde{q}(t)) + v(t)\, Y(\tilde{q}(t)) \tag{4}$$

and the derivative of the heading angle $v(t) = \alpha'(t) \in \mathbb{R}$ is called the *accessory control*. Denoting $\tilde{z} = (\tilde{q}, \tilde{p})$, $\tilde{p} = (p, p_\alpha)$, we define the extended pseudo-Hamiltonian by

$$\widetilde{H}(\tilde{z}, v) = \langle \tilde{p}, X(\tilde{q}) + v\, Y(\tilde{q}) \rangle + p^0.$$

By [4, Chapter 6], in this representation, geodesic curves become *singular trajectories* of (4).

Recall that the Lie bracket of two vector fields U, V is defined by

$$[U,V](\tilde{q}) = \frac{\partial U}{\partial \tilde{q}}(\tilde{q})\, V(\tilde{q}) - \frac{\partial V}{\partial \tilde{q}}(\tilde{q})\, U(\tilde{q})$$

and is related to the Poisson bracket by $\{H_U, H_V\}(\tilde{z}) = \mathrm{d}H_U(\tilde{z}) \cdot \overrightarrow{H}_V(\tilde{z})$ by the relation

$$\{H_U, H_V\}(\tilde{z}) = \langle \tilde{p}, [U,V](\tilde{q})\rangle,$$

where H_U, H_V are the Hamiltonian lifts of U and V. It is easy to check that

$$\frac{\mathrm{d}}{\mathrm{d}t}\frac{\partial \widetilde{H}}{\partial v}\bigg|_{(\tilde{q},\tilde{p},v)} = \langle \tilde{p}, [Y,X](\tilde{q})\rangle,$$
$$\frac{\partial}{\partial v}\frac{\mathrm{d}^2}{\mathrm{d}t^2}\frac{\partial \widetilde{H}}{\partial v}\bigg|_{(\tilde{q},\tilde{p},v)} = \langle \tilde{p}, [[Y,X],Y](\tilde{q})\rangle.$$

Proposition 1. *Defining*

$$D = \det(Y, [Y,X], [[Y,X],Y]),$$
$$D' = \det(Y, [Y,X], [[Y,X],X]),$$
$$D'' = \det(Y, [Y,X], X),$$

any extremal control v is given by the feedback

$$v(t) = v_s(\tilde{q}(t)) = -\frac{D'(\tilde{q}(t))}{D(q(t))} \tag{5}$$

and the geodesics are solutions of

$$\frac{\mathrm{d}\tilde{q}}{\mathrm{d}t}(t) = X(\tilde{q}(t)) + v_s(\tilde{q}(t))\, Y(\tilde{q}(t)) = X_s(\tilde{q}(t)). \tag{6}$$

Moreover:

- *hyperbolic geodesics are in the region where $DD'' > 0$;*
- *elliptic geodesics are in the region where $DD'' < 0$;*
- *abnormal (or exceptional) geodesics are in the region where $D'' = 0$.*

Proof. We refer to [4, Sec. 3.4]. A singular control-trajectory pair $(\tilde{q}, v)$ satisfies

$$H_Y(\tilde{z}) = \{H_Y, H_X\}(\tilde{z}) = 0$$
$$\{\{H_Y, H_X\}, H_X\}(\tilde{z}) + v\,\{\{H_Y, H_X\}, H_Y\}(\tilde{z}) = 0$$

and this leads to

$$\begin{aligned} 0 &= \langle \tilde{p}, Y(\tilde{q})\rangle = p_\alpha, \\ 0 &= \langle \tilde{p}, [Y,X](\tilde{q})\rangle, \\ 0 &= \langle \tilde{p}, [[Y,X],X](\tilde{q}) + v\,[[Y,X],Y](\tilde{q})\rangle. \end{aligned}$$

Hence, since $\tilde{p} \in \mathbb{R}^3 \setminus \{0\}$, $\tilde{p}$ can be eliminated. Moreover, every geodesic is strict and $D(\tilde{q})$ is never vanishing. Hence, the geodesic control $v(\cdot)$ is given by (5). The geodesic classification follows. □

2.3 Feedback pseudo-group G_f and singularity analysis

Given a pair (X, Y) of vector fields, the set of triples (φ, α, β), where φ is a local diffeomorphism and where $u = \alpha(x) + \beta(x)\, u'$, with $\beta \neq 0$, is a feedback, acts on (X, Y). This action induces the pseudo-feedback group G_f.

Theorem 1 ([4]). *Let λ_s be the mapping which yields for each pair (X, Y) the dynamics (6). Then λ_s is a covariant mapping, i.e., the following diagram is commutative:*

$$\begin{array}{ccc} (X,Y) & \xrightarrow{\lambda_s} & X_s \\ {\scriptstyle G_f}\big\downarrow & & \big\downarrow{\scriptstyle G_f} \\ (X',Y') & \xrightarrow{\lambda_s} & X'_s \end{array}$$

Proof. The proof follows from straightforward computations on the determinants D, D'. □

Definition 1. *We define the collinear set by* $\mathscr{C} = \{q \mid \exists \alpha,\ F_0(q) + \cos\alpha\, F_1(q) + \sin\alpha\, F_2(q) = 0\}$.

Proposition 2.

1. *The geodesic curves are immersed curves outside of the collinear set.*
2. *Only abnormal geodesics can be non-immersed curves when meeting the collinear set.*

Proof. This comes from the relation between the set $\{\|F_0\|_g = 1\}$ and the collinear set. Indeed take $q_0 \in \{\|F_0\|_g = 1\}$, then there exists α_0 such that:

$$F_0(q_0) + \cos\alpha_0 F_1(q_0) + \sin\alpha_0 F_2(q_0) = 0$$

so that for the dynamics $\dot{q} = 0$ when meeting the collinear set. If $q(t)$ is a geodesic, one has $p_\alpha = 0$ and the Hamiltonian vanishes. It is constant along any geodesic, hence the geodesic is abnormal. □

Singularity analysis. A remarkable property of the geodesics already observed in the historical example (see [10]) is the existence of a cusp singularity for the abnormal curves when meeting the set $\{\|F_0\|_g = 1\}$. This serves as a model to construct a normal form to analyze in a general framework this situation [6].

Theorem 2. *Let $q_1 \in \{\|F_0\|_g = 1\}$. Let σ be a geodesic such that $q_1 = \sigma(0)$ is not an immersion at $t = 0$ and α_1 be the heading at $t = 0$. Then the geodesic σ has an abnormal extremal lift and if $\alpha(\cdot)$ is the heading angle we have only two situations:*

1. *If $\dot{\alpha}(0) \neq 0$ and $\{\|F_0\|_g = 1\}$ is regular at q_1, then σ has a semi-cubical cusp at q_1.*
2. *If $\dot{\alpha}(0) = 0$, then $\tilde{q}_1 = (q_1, \alpha_1)$ is a singular point of the dynamics (6) and the spectrum of the linearized dynamics is a feedback invariant.*

Proof. The complete proof is provided in [6] but we indicate the main idea of the proof. The problem is local in a neighborhood of q_1 and we can choose coordinates (x, y) in which $q_1 = (0, 0)$, $F_0 = -\partial/\partial x$ and $g = a(x, y)\left(\mathrm{d}x^2 + \mathrm{d}y^2\right)$ (*isothermal form*). Moreover, F_0 and F_1 have opposite directions. It then suffices to expand $F_0 = b(x, y)\partial/\partial x + c(x, y)\partial/\partial y$ and g at $(0, 0)$ to evaluate $\{\|F_0\|_g = 1\}$, D, D' and D''. □

The following theorem describes the optimality properties of the geodesics in a *conic neighborhood* of the small-time reference abnormal arc σ_a.

Theorem 3. *Assume that the reference abnormal arc has a semi-cubical cusp at $t = 0$, then for t small enough:*

1. *The abnormal arc is minimal time from $\sigma_a(t) = q_0$, $t < 0$, until $\sigma_a(0) = q_1$.*
2. *Hyperbolic geodesics starting from q_0 in a conic neighborhood of the abnormal arc are self-intersecting and are minimal time up until their second intersection with the abnormal arc, this point being excluded.*
3. *Elliptic geodesics starting from q_0 in a conic neighborhood of the reference abnormal are maximal time and are confined in the weak current domain $\{\|F_0\|_g < 1\}$.*

The behaviors of the geodesics described in Theorem 3 are represented on Figure 1.

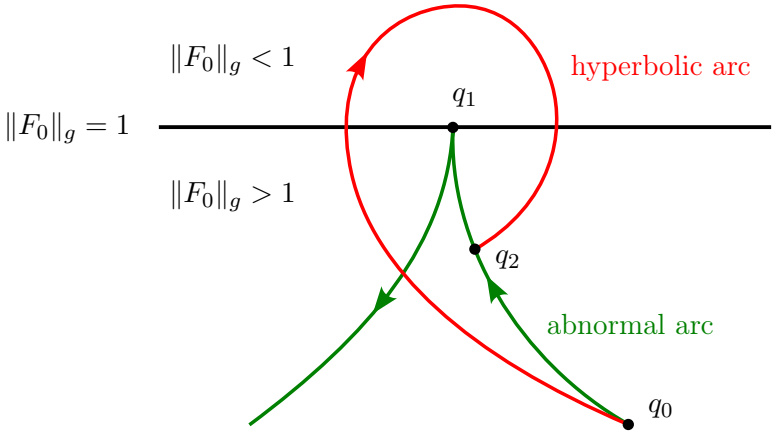

Figure 1: Cusp singularity and self-intersecting arcs in a neighborhood of $\|F_0\|_g = 1$.

Remark 1. In particular, within the framework of Theorem 3, it follows that the minimal control time function is not continuous near the abnormal arc. This implies a loss of local controllability along this arc.

2.4 Optimality analysis

Let $\tilde{\sigma}$ be a reference geodesic defined on $[0, t_f]$, $\tilde{\sigma}(t) = (q(t), \alpha(t))$, $\tilde{\sigma}(0) = (q_0, \alpha_0)$ with q_0 being a fixed initial point. The *first conjugate time* along $\tilde{\sigma}$ is the first time t_{1c} at which $\tilde{\sigma}$ ceases to be minimizing, compared with geodesic curves $\tilde{q}$ such that $\tilde{q}(0) = (q_0, \tilde{\alpha}_0)$, $|\alpha_0 - \tilde{\alpha}_0$ small enough, that is in a conic neighborhood of the reference geodesic. Fixing q_0, the set of first conjugate points is called the *conjugate locus* $C(q_0)$. The *cut time* t_c is the first time at which σ ceases to be (globally) optimal. The set of cut points is called the *cut locus* $\Sigma(q_0)$. Fixing q_0 and q_1 on M, we denote by $T(q_0, q_1)$ the *minimal time value function*, that is, $T(q_0, q_1) = \min t_f$ among all trajectories $q(\cdot)$ such that $q(0) = q_0$ and $q(t_f) = q_1$. The problem is said to be *geodesically complete* if for all $q_0, q_1 \in M$ there exists a minimal time geodesic joining q_0 to q_1.

Proposition 3.

1. *Cusp points correspond to conjugate points along abnormal geodesics.*
2. *In a neighborhood of a cusp point q_1 the time transfer from the point q_0 to q_2 (see Figure 1) is larger along the hyperbolic arc than along the abnormal arc.*

Proof. The first assertion comes from Theorem 3. The second assertion is obtained by straightforward computations (see [6] for details). □

2.5 Liouville-Mineur-Arnold theorem and classification of geodesics in the Riemannian case

We recall the standard Liouville-Mineur-Arnold theorem which is crucial to understand the Hamiltonian dynamics (see [2]).

Theorem 4. *Let (M,ω) be a 4-dimensional symplectic manifold. Let H and G be two smooth functions such that $\{H,G\}=0$, $\overrightarrow{H}$, $\overrightarrow{G}$ are complete, and H, G are functionally independent. Consider the level surfaces $T_\xi=\{H=\xi_1,\ G=\xi_2\}$ for any $\xi=(\xi_1,\xi_2)$. If T_ξ is connected and compact, then:*

1. *each T_ξ is diffeomorphic to a 2-dimensional torus T^2 called a* Liouville torus*;*
2. *the Liouville foliation is locally trivial and there exist symplectic coordinates (I,φ) called* action-angle variables *in which the dynamics of $\overrightarrow{H}$ become*

$$\frac{\mathrm{d}I_k}{\mathrm{d}t}=0,\quad \frac{\mathrm{d}\varphi_k}{\mathrm{d}t}=\alpha_k(I),\quad k=1,2,$$

and the motion is quasi-periodic.

Application to the Riemannian case on the 2-sphere of revolution $\mathbf{M=S^2}$. Consider the family of metrics on S^2 given by $g_\lambda=\mathrm{d}r^2+m_\lambda^2(r)\,\mathrm{d}\theta$ with

$$m_\lambda^2(r)=\frac{\sin^2 r}{1-\lambda\sin^2 r}$$

where $\lambda\in[0\,,1)$ is an homotopic parameter, $\lambda=0$ corresponds to the *round sphere* and $\lambda=1$ is the *Grushin case*, which is singular at the equator $r=\pi/2$. They were introduced in [3]. The case $\lambda=4/5$ corresponds to the *averaged Kepler case*.

In the Riemannian case, minimizing the length is equivalent to minimize the energy so that from the Pontryagin maximum principle we infer the following result.

Proposition 4. *Geodesics are solutions of the Hamiltonian dynamics given by the Hamiltonian function*

$$H=\frac{1}{2}\left(H_1^2+H_2^2\right),$$

with $H_i=\langle p,F_i\rangle$, for $i=1,2$ and $F_1=\dfrac{\partial}{\partial r}$, $F_2=\dfrac{1}{m(r)}\dfrac{\partial}{\partial\theta}$. By homogeneity, one can parametrize by arc length: $H=1/2$, so that for the geodesics the r-dynamics is solution of

$$\left(\frac{\mathrm{d}r}{\mathrm{d}t}\right)^2=1-V(r,p_\theta) \tag{7}$$

where $V(r,p_\theta)=1-\frac{p_\theta^2}{m^2(r)}$ is the potential*, and p_θ is constant (Clairaut relation). The θ-dynamics satisfies*

$$\frac{\mathrm{d}\theta}{\mathrm{d}t}=\frac{p_\theta}{m^2(r)}. \tag{8}$$

The metric is reflectionally symmetric with respect to the equator $r=\pi/2$ ($m(r)=m(\pi-r)$) and every geodesic intersects the equator so that the dynamics can be integrated with $q(0)=(\pi/2,0)$.

Proposition 5. *One can assume that $p_\theta \in [0\,, m(\pi/2)]$. Geodesics are given by:*

- *the equator solution $r = \pi/2$ for $p_\theta = m(\pi/2)$;*
- *the meridian solution for $p_\theta = 0$;*
- *geodesics which are quasi-periodic.*

Proof. To integrate, one can substitute r by $\pi/2 - r$, so that the equator is identified to $r = 0$, while $m(r)$ is substituted by $m(r) = \cos^2 r/(1 - \lambda \cos^2 r)$. Starting from the equator with $0 < p_\theta < 1/m(r)$, using the ascending branch of (7), r oscillates periodically between $-r^+ \leq r \leq r^+$ where r^+ is the positive root of $V(r, p_\theta) = 1$. This leads to r-periodic geodesics.

The second step is to integrate by quadrature the equation (8). Altogether, this gives quasi-periodic solutions which are either periodic or dense in a 2-dimensional torus. □

Hence, the Riemannian case associated to the family of metrics g_λ fits in the geodesic frame of the Liouville-Mineur-Arnold theorem, provided that the homogeneity $H(\lambda p) = \lambda^2 H(p)$ is taken into account. This opens the way to analyze the Zermelo navigation problem in the case of revolution, based on the mechanical framework, which we do next.

2.6 Classification of the geodesics for Zermelo navigation problems on the two-sphere for revolution metrics

Motivated by the applications, we restrict our study to metrics $m_\lambda(r) = \sin^2 r/(1-\lambda \sin^2 r)$ where $\lambda \in [0\,, 1]$. For $\lambda = 1$ this corresponds to the singular Grushin case. The current takes the form

$$F_0(q) = \mu_1(r)\frac{\partial}{\partial r} + \mu_2(r)\frac{\partial}{\partial \theta}$$

and the maximized Hamiltonian is

$$M = p_r\, \mu_1(r) + p_\theta\, \mu_2(r) + \|p\|_g + p^0 \tag{9}$$

with $\|p\|_g = \sqrt{p_r^2 + p_\theta^2/m^2(r)}$. Moreover, one has $M = 0$ and the hyperbolic, elliptic and abnormal cases correspond respectively to $p^0 < 0$, $p^0 > 0$ and $p^0 = 0$. Using the Pontryagin maximum principle, we get the following result.

Proposition 6. *The geodesics dynamics are the solutions of*

$$\left.\begin{aligned} \frac{\mathrm{d}r}{\mathrm{d}t} &= \mu_1(r) + \frac{p_r}{\|p\|_g} \\ \frac{\mathrm{d}p_r}{\mathrm{d}t} &= -p_r\, \mu_1'(r) - p_\theta\, \mu_2'(r) - \frac{p_\theta^2}{\|p\|_g}\frac{m'(r)}{m^3(r)} \end{aligned}\right\} \tag{10}$$

$$\frac{\mathrm{d}\theta}{\mathrm{d}t} = \mu_2(r) + \frac{p_\theta}{\|p\|_g}\frac{1}{m^2(r)} \tag{11}$$

and $p_\theta =$ constant.

Definition 2. *Fixing p_θ, the Hamiltonian dynamics (10) associated to M, restricted to the (r, p_r)-space, is called the* Morse-Reeb dynamics.

The main point of the study of the geodesics is to analyze the behaviors of the Morse-Reeb dynamics. To fix the geometric frame we recall next the Morse-Reeb classification of the orbits.

2.6.1 A recap of Reeb classification of 2d-Hamiltonian systems

In this section we present a brief recap of the construction in the 2D Hamiltonian case to deduce our construction, the presentation being based on references [1, 2, 15]. Without losing any generality, one can assume that the 2d-symplectic manifold is the cotangent space T^*M of a 1d-manifold M. Let $z = (p, q)$ be canonical (Darboux) coordinates. Let $H(p, q)$ be an Hamiltonian where $q \in M$ and $\alpha = p\,dq$ is the Liouville form on T^*M and the 2-form ω is the derivative $d\alpha$. We assume that $O = (0, 0)$ is an equilibrium point of the dynamics so that $\mathrm{D}H(O) = 0$. Expanding in the jet-space at O, we note H_2 the quadratic term of the Hamiltonian.

Thanks to Williamson [20], the computations of normal (Jordan) forms in the $2n$-case are reduced to the action of the symplectic group $\mathrm{Sp}(n, \mathbb{R})$. Note that from [13] each symplectomorphism is locally represented by a generating function. Among those, each diffeomorphism $Q = f(q)$ with $\partial f/\partial q$ invertible can be extended to a symplectic transformation with generating mapping

$$S(q, P) = f(q)^{\mathrm{T}} P$$

so that

$$p = \left(\frac{\partial f}{\partial q}(q)\right)^{\mathrm{T}} P, \quad Q = f(q).$$

The diffeomorphism is denoted φ and the induced symplectomorphism $\overrightarrow{\varphi}$. It is called a *Mathieu transformation*.

Note that in 2d-case $\mathrm{Sp}(1, \mathbb{R}) = \mathrm{Sl}(2, \mathbb{R})$ and the canonical form coincides with the volume form. From generic point of view we have two situations. In symplectic coordinates the quadratic Hamiltonian is given by:

- Elliptic case: $H_2(P, Q) = \frac{1}{2}\lambda(P^2 + Q^2)$;
- Hyperbolic case: $H_2(P, Q) = \frac{1}{2}\lambda(PQ)$.

Lemma 1. *In the previous computations the only linear symplectic invariant is λ which corresponds respectively to the spectrum of $\overrightarrow{H}_2$ that is $\pm i\lambda$ in the elliptic case and $\pm\lambda$ in the hyperbolic case.*

The second step following [1] is to construct the Birkhoff normal form at order m where the polynomic term of the Taylor expansion of H is truncated at order $2m$ and writes

$$H_m = h(x),$$

where $h(x)$ is a polynomial of degree m depending on:

- Elliptic case: $x = (P^2 + Q^2)$;
- Hyperbolic case: $x = PQ$.

This normal form is obtained using the Poincaré-Dulac method reducing the Hamiltonian by successive compositions of symplectomorphisms close to the identity and parametrized by their generating functions, see [13] for an algorithmic description of the method. This computation leads to compute a sequence of symplectic invariants in the jet space, generalizing the spectrum λ of the quadratic part.

Lemma 2. *Using the previous calculation, one gets a sequence of symplectic invariants which are the coefficients of the Taylor series of $h(x)$ at $x = 0$.*

Reeb classification. The previous computation leads to introduce the Reeb classification. The Birkhoff normal leads to compute with an arbitrary accuracy the level sets of H which are in the coordinates (P, Q):

- Elliptic case: concentric circles;
- Hyperbolic case: they are identified to hyperbolas.

Let us introduce the orbits as level sets of H which form a one-dimensional foliation of the symplectic space identified to T^*M. Two points of the space are called equivalent if they belong to the same orbit and we denote by $\sim$ this equivalence relation. The Reeb space denoted $\mathscr{R}$ is the the topological quotient space $T^*M/\sim$. In this construction one can define a measure μ on the quotient space by projecting the canonical measure on T^*M on the quotient, using the canonical projection π.

Using this approach the singular points of the dynamics associated to $\overrightarrow{H}$ are the solutions of $\mathrm{D}H = 0$, that is the singular orbits. One can use [15] for a complete description of this construction to classify globally the level sets of the Hamiltonian H and the introduction of the Reeb graph to encode this construction.

2.6.2 Extension of the Morse-Reeb classification to the Zermelo case

Roughly spoken it amounts to classifiy the Hamiltonian dynamics from (9) restricting to Mathieu symplectomorphisms in the (r, p_r) space. It has to be adapted using the following obvious property.

Lemma 3. *The Hamiltonians M satisfies $M(\lambda p, \lambda p^0) = \lambda M(p, p^0)$ for $\lambda > 0$.*

Introduction of the potential. From (10), one has:

$$p_r^2 + \frac{p_\theta^2}{m^2(r)} = \left(p^0 + p_r\,\mu_1(r) + p_\theta\,\mu_2(r)\right)^2. \tag{12}$$

and from the dynamics (10), we deduce:

$$\left(\frac{\mathrm{d}r}{\mathrm{d}t} - \mu_1(r)\right)^2 = 1 - \frac{p_\theta^2}{m^2(r)(p^0 + p_r\,\mu_1(r) + p_\theta\,\mu_2(r))^2}. \tag{13}$$

In particular, eq. (13) generalizes the eq. (7) of the Riemannian case, in the case of a parallel current.

Proposition 7. *In the case of a parallel current: $\mu_1(r) = 0$, the r-dynamics is described by the mechanical system:*

$$\left(\frac{\mathrm{d}r}{\mathrm{d}t}\right)^2 = 1 - V(r, p_\theta) \tag{14}$$

where

$$V(r, p_\theta) = \frac{p_\theta^2}{m^2(r)(p^0 + p_\theta\,\mu_2(r))^2}$$

is the potential.

Hence, in particular we have [5].

Proposition 8. *In the case of a parallel current, an equator $r = r^*$ constant solution of the geodesic dynamics corresponds to a singular point of the Morse-Reeb dynamics with $p_r^* = 0$. The pair (r^*, p_θ^*) is given by solving $V = 1$ and $\partial V/\partial r = 0$. The associated singularity is hyperbolic (resp., elliptic) if and only if $\frac{\partial^2 V}{\partial r^2} < 0$ (resp., $\frac{\partial^2 V}{\partial r^2} > 0$). A separatrix geodesic such that $r(t) \to r^*$ as $t \to \infty$ is necessarily associated to an hyperbolic equator (r^*, p_θ^*).*

Definition 3. *In the case of parallel current, on the two-sphere of revolution, the elliptic case splits into short r-periodic orbits contained in one hemisphere and long periodic orbits crossing the equatorial plane.*

The case of a general current. If $\mu_1(r)$ is not identically zero, p_r occurs in the right-hand-side of equation (13) and hence the r-dynamics has to be analyzed in a more general framework. We proceed as follows. One can write (12) as a second order polynomial

$$P(p_r) = a\,p_r^2 + b\,p_r + c = 0 \tag{15}$$

with

$$a = 1 - \mu_1^2(r), \quad b = -2\mu_1(r)(p^0 + p_\theta \mu_2(r)), \quad c = \frac{p_\theta^2}{m^2(r)} - (p^0 + p_\theta \mu_2(r))^2.$$

The discriminant of the polynomial P is given by

$$\Delta = b^2 - 4ac = 4(\mu_1^2(r) - 1)\frac{p_\theta^2}{m^2(r)} + 4(p^0 + p_\theta \mu_2(r))^2.$$

The r-dynamics writes

$$\frac{\mathrm{d}r}{\mathrm{d}t} = \mu_1 + \frac{p_r}{\|p\|_g}.$$

Taking the square, one gets a second order equation:

$$P'(p_r) = a' p_r^2 + b' p_r + c' = 0 \tag{16}$$

with

$$a' = a = 1 - \mu_1^2, \quad b' = 0, \quad c' = -\frac{p_\theta^2}{m^2}\,\mu_1^2.$$

Hence, the Morse-Reeb classification amounts to analyze the orbits solution of (15) and the dynamics on each orbit is given by (10). In particular, one needs to solve $P = P' = 0$ and we introduce the following [19].

Definition 4. *The resultant $R(P, P')$ of the two polynomial is given by the determinant of the 4×4 matrix*

$$\begin{pmatrix} a & 0 & a & 0 \\ b & a & 0 & a \\ c & b & c' & 0 \\ 0 & c & 0 & c' \end{pmatrix}.$$

Computations. We fix p_θ and we compute the roots of $R = 0$. Details are given next in the Lindblad case where practically, the *discrete symmetric group* has to be used to simplify the computations.

2.7 A case study with vertical current

2.7.1 Lindblad equation and simplified current.

The dynamics in the Euclidean coordinates $q = (x, y, z)$ are given by

$$\begin{aligned} \frac{\mathrm{d}x}{\mathrm{d}t} &= -\Gamma x + u_2 z, \\ \frac{\mathrm{d}y}{\mathrm{d}t} &= -\Gamma y - u_1 z, \\ \frac{\mathrm{d}z}{\mathrm{d}t} &= \gamma_- - \gamma_+ z + u_1 y - u_2 x. \end{aligned}$$

The set of parameters $\Lambda = (\Gamma, \gamma_-, \gamma_=)$ is such that: $\Gamma \geqslant \gamma_+/2 > 0$, $\gamma_+ \geqslant \gamma_-$ so that the *Bloch ball*: $|q| \leqslant 1$ is invariant for the dynamics. The parameter Γ is called the *dephasing rate*. We have $\gamma_+ = \gamma_{12} + \gamma_{21}$, $\gamma_- = \gamma_{12} - \gamma_{21}$, where γ_{12}, γ_{21} are the *population relaxation rates*.

The control is the *complex Rabi laser frequency*: $u = u_1 + iu_2$ and we assume that $|u| \leqslant 1$. Denoting by

$$G_1 = \begin{pmatrix} 0 & 0 & 0 \\ 0 & 0 & -1 \\ 0 & +1 & 0 \end{pmatrix}, \quad G_2 = \begin{pmatrix} 0 & 0 & +1 \\ 0 & 0 & 0 \\ -1 & 0 & 0 \end{pmatrix},$$

G_1 and G_2 correspond respectiveley to rotations around the axis Ox and Oy. The induced metric on the 2-sphere is the Grushin metric.

In order to simplify Lie brackets computations, the original system can be written as the control-affine system

$$\frac{\mathrm{d}q}{\mathrm{d}t} = (G_0 q + v_0) + u_1 G_1 q + u_2 G_2 q$$

with

$$G_0 = \begin{pmatrix} -\Gamma & 0 & 0 \\ 0 & -\Gamma & 0 \\ 0 & 0 & -\gamma_+ \end{pmatrix}, \quad v_0 = \begin{pmatrix} 0 \\ 0 \\ \gamma_- \end{pmatrix},$$

which corresponds to the action of the semi-direct product $\mathrm{Gl}(3,\mathbb{R}) \oplus_s \mathbb{R}^3 \subset \mathrm{Gl}(4,\mathbb{R})$ on the $\mathbb{R}^3$-space with coordinates q identified to the affine space $(1, q)$. The Lie bracket being given by

$$[(a, A), (b, B)] = (Ab - Ba, AB - BA).$$

Using spherical coordinates $x = \rho \sin r \cos\theta$, $y = \rho \sin r \sin\theta$, $z = \rho \cos r$, and using a control feedback preserving the Euclidean norm, the system writes:

$$\frac{\mathrm{d}\rho}{\mathrm{d}t} = \gamma_- \cos r - \rho(\gamma_+ \cos^2 r + \Gamma \sin^2 r), \tag{17}$$

$$\frac{\mathrm{d}r}{\mathrm{d}t} = -\frac{\gamma_- \sin r}{\rho} + \frac{\sin 2r}{2}(\gamma_+ - \Gamma) + v_2, \tag{18}$$

$$\frac{\mathrm{d}\theta}{\mathrm{d}t} = -\cot r \, v_1. \tag{19}$$

Susch a system is defined in the Bloch ball which is 3-dimensional while the control $v = (v_1, v_2)$ is valued in the 2-dimensional unit ball. Hence, it corresponds to sub-Finsler geometric problem. It will define a Zermelo type navigation problem in the so-called integrable case where γ_- is interpreted as a dissipation parameter setting $\gamma_- = 0$.

The analysis of the orbits fits in the previous section except that singularities occur on the equator since the metric g is singular, in particular the equator is not a solution. Note that we can take the homotopy parameter $\lambda < 1$, $\lambda \sim 1$.

Lemma 4. *If $\gamma_- = 0$, then, the current is vertical and is zero at the equator $r = \pi/2$ and is maximal in each hemisphere at $r = \pi/4$, $\pi/4 + \pi/2$. It can be compensated by a feedback provided $|\gamma_+ - \Gamma| < 2$, thus defining a sub-Finsler problem.*

If we set: $\tilde{r} = \ln \rho$, so that the first equation of (17) can be integrated by quadrature and becomes a cyclic variable for the dynamics. This gives in fine two cyclic variables $\tilde{r}$ and θ. Introducing the adjoint vector $p = (p_{\tilde{r}}, p_r, p_\theta)$ the leading maximized Hamiltonian writes

$$M = -(\gamma_+ \cos^2 r + \Gamma \sin^2 r)\, p_{\tilde{r}} + \frac{\sin 2r}{2}(\gamma_+ - \Gamma)\, p_r + \sqrt{p_r^2 + p_\theta^2 \cot^2 r} + p^0.$$

Since $p_{\tilde{r}}$ is constant, this gives a family like of Zermelo navigation problems on the 2-sphere of revolution associated to the Grushin metric given in the dual form by:

$$\|p\|_g = \sqrt{p_r^2 + p_\theta^2 \cot^2 r}.$$

The problem is a test bed case to develop in more details the Morse-Reeb classification, using specific symmetries.

Lemma 5.

– *One has the following symmetries.*

1. *Since the current is vertical ($\mu_2 = 0$), one has either $\frac{\mathrm{d}\theta}{\mathrm{d}t} \equiv 0$ if and only if $p_\theta = 0$ and if $p_\theta \neq 0$, $\frac{\mathrm{d}\theta}{\mathrm{d}t}$ is not vanishing. Hence, we can assume $p_\theta \geqslant 0$.*
2. *The Hamiltonian M is invariant for the central symmetry $(r, p_r) \mapsto (\pi - r, -p_r)$.*

In particular, one has:

Lemma 6. *Due to the central symmetry, r-periodic geodesics split into short periodic orbits contained in one hemisphere and long periodic orbits crossing the equator.*

Lemma 7. *Since μ_1 is not identically zero, the set of solutions $\{r \mid 1 - \mu_1^2(r) = 0\}$ forms* barriers *and with $\mu_1(r) = \sin 2r\,(\gamma_+ - \Gamma)/2$, this leads if $|\gamma_+ - \Gamma| > 2$ to two barriers in each hemisphere, in which the dynamics is trapped.*

Lemma 8. *Let $t \mapsto (r(t), p_r(t))$ be an orbit of the dynamics so that $|p_r(t)| \to +\infty$ as $t \to +\infty$. Then, the supporting orbit is not compact and moreover $r(t) \to r_0$ as $|t| \to +\infty$, where r_0 is a barrier.*

2.7.2 A simplified model for the complete analysis and numerical simulations

The study of the Lindblad case comes down to the analysis of the family of systems on the 2D sphere with revolution metric given by

- the vertical current: $F_0 = \delta \sin 2r \frac{\partial}{\partial r}$, where δ is a parameter.
- the metrics $m_\lambda^2(r) = \sin^2 r/(1 - \lambda \sin^2 r)$ where $\lambda \in [0\,, 1)$ is a homotopic parameter.

The current is zero at the poles and at the equator and $\|F_0\|_g$ is maximal at $r = \pi/4$, $\pi/4 + \pi/2$. The Finsler case corresponds to $|\delta| < 1$. In each hemisphere the two barriers coincide in the case $|\delta| = 1$ and the dynamics can be studied locally by expanding $\sin 2r$ at $r = \pi/4$ to describe the transition. For the case $|\delta| > 1$, the controllability property can be studied using the barriers since the current is pointing either toward the poles or toward the equator.

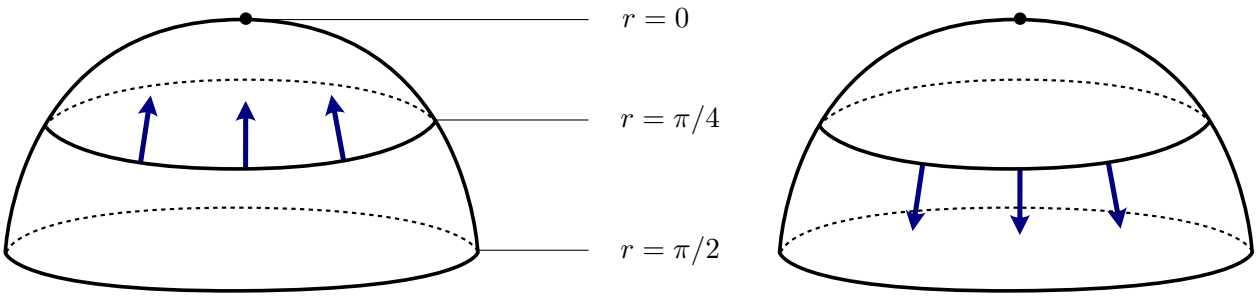

Figure 2: Representation of the current in the North hemisphere. On the left, $\delta > 0$ while on the right $\delta < 0$.

Computations of the singularities of the dynamics. We have $M = p_r\mu(r) + \|p\|_g + p^0$, with $\|p\|_g = \sqrt{p_r^2 + p_\theta^2/m_\lambda^2(r)}$, $\mu(r) = \delta \sin 2r$ and $m_\lambda^2(r) = \sin^2 r/(1 - \lambda \sin^2 r)$. The dynamics reads

$$\frac{\mathrm{d}r}{\mathrm{d}t} = \frac{\partial M}{\partial p_r} = \mu(r) + \frac{p_r}{\|p\|_g}$$
$$\frac{\mathrm{d}p_r}{\mathrm{d}t} = -\frac{\partial M}{\partial r} = -p_r\,\mu'(r) + \frac{p_\theta^2}{m_\lambda^3(r)}\frac{m_\lambda'(r)}{\|p\|_g}.$$

Singularity analysis. We distinguish between two cases:

- Case $p_r = 0$. We must solve $\mu(r) = 0$ and $p_\theta m_\lambda'(r) = 0$. Since $p \neq 0$, one has $p_\theta \neq 0$ and we get the solution $\mu(r) = m_\lambda'(r) = 0$ which corresponds to the equator $r = \pi/2$.
- Case $p_r \neq 0$. They correspond to additional singularities whose determination is crucial in relationship with short periodic orbits since every solution has to encircle a singular point. From the previous equation, they exist only in the weak current domain where $\|F_0\|_g \leq 1$. In the round case $m_\lambda' = 0$ we must have $\mu'(r) = 0$.

Existence of long periodic orbits.

Lemma 9. *If the level set $M = 0$ is compact, without singular point and has a central symmetry with respect to the point $(r, p_r) = (\pi/2, 0)$, then it contains a periodic trajectory (r, p_r) of period T, and if $p_r^\pm(0)$ are distinct then we have two distinct geodesics $q^+(\cdot)$ and $q^-(\cdot)$ starting from the same point and intersecting with the same length $T/2$ at a point such that $r(T/2) = \pi - r(0)$.*

Proof. The proof is similar to the Riemannian case to construct long periodic orbits starting from the equator $r(0) = \pi/2$. Indeed, consider the equation (15) and assume that $\Delta > 0$. Let $p_r^\pm$ be the two distinct roots and let $q^\pm(\cdot) = (r^\pm(\cdot), \theta^\pm(\cdot))$ be the two corresponding distinct geodesics with initial condition $p^\pm(0)$, starting from $(\pi/2, 0)$ and on the same level set $M + p^0 = 0$. Using the central symmetry, $r^\pm$ are T-periodic and moreover $r^+(T/2) = r^-(T/2)$, $\theta^+(T/2) = \theta^-(T/2)$. □

Corollary 1. *Long r-periodic orbits correspond to quasi-periodic geodesics preserving quasi-periodic of the Riemannian case.*

Carathéodory-Zermelo-Goh geodesic representation. We have

$$X = (\mu(r) + \cos\alpha)\frac{\partial}{\partial r} + \frac{\sin\alpha}{m(r)}\frac{\partial}{\partial\theta}, \quad Y = \frac{\partial}{\partial\alpha},$$

in coordinates $\tilde{q} = (r, \theta, \alpha)$, and we compute

$$[Y, X](\tilde{q}) = \sin\alpha\frac{\partial}{\partial r} - \frac{\cos\alpha}{m(r)}\frac{\partial}{\partial\theta},$$

and

$$\begin{aligned}
[[Y, X], Y](\tilde{q}) &= \cos\alpha\frac{\partial}{\partial r} + \frac{\sin\alpha}{m(r)}\frac{\partial}{\partial\theta},\\
[[Y, X], X](\tilde{q}) &= -\mu'\sin\alpha\frac{\partial}{\partial r} + \frac{m'}{m}(1 + \mu\cos\alpha)\frac{\partial}{\partial\theta}.
\end{aligned}$$

Hence,

$$\begin{aligned}
D(\tilde{q}) &= \frac{1}{m(r)},\\
D''(\tilde{q}) &= \frac{1}{m(r)}(1 + \mu(r)\cos\alpha)
\end{aligned}$$

and

$$\begin{aligned}
D'(\tilde{q}) &= \sin\alpha\frac{m'}{m^2}(1 + \mu\cos\alpha) - \frac{\mu'}{m}\sin\alpha\cos\alpha\\
&= \frac{\sin\alpha}{m}\left(\frac{m'}{m}(1 + \mu\cos\alpha) - \mu'\cos\alpha\right).
\end{aligned}$$

The dynamics is

$$\begin{aligned}
\frac{\mathrm{d}r}{\mathrm{d}t} &= \mu(r) + \cos\alpha,\\
\frac{\mathrm{d}\theta}{\mathrm{d}t} &= \frac{\sin\alpha}{m(r)},\\
\frac{\mathrm{d}\alpha}{\mathrm{d}t} &= -\frac{D'(\tilde{q})}{D(\tilde{q})}.
\end{aligned}$$

The representation is interesting because it encodes the geometric objects. In particular, one can compare with the case study of the historical example of [5].

Proposition 9. *In the case of a vertical current $\mu(r)$:*

1. *The collinear set is the barrier given by $\mu(r) + \cos\alpha = \sin\alpha = 0$.*
2. *The limit abnormal arcs in strong current domains satisfy $\mu(r)\, m(r)\sin\alpha + 1 = 0$.*
3. *D' vanishes along the collinear set.*

3 Applications

3.1 Numerical simulations for the simplified Lindblad model

We consider the simplified model of the Lindblad system. We first set $\delta = 1.25$ and $r_0 = \pi/2$. We can observe on Figure 3 the geodesic flow. One can see that the flow is trapped between the two regions of strong current since in the North hemisphere, the current is pointing down while in the South hemisphere, it is pointing up. We can compute the cut locus which is simply given by an arc of the initial meridian (by symmetry), see Figure 4.

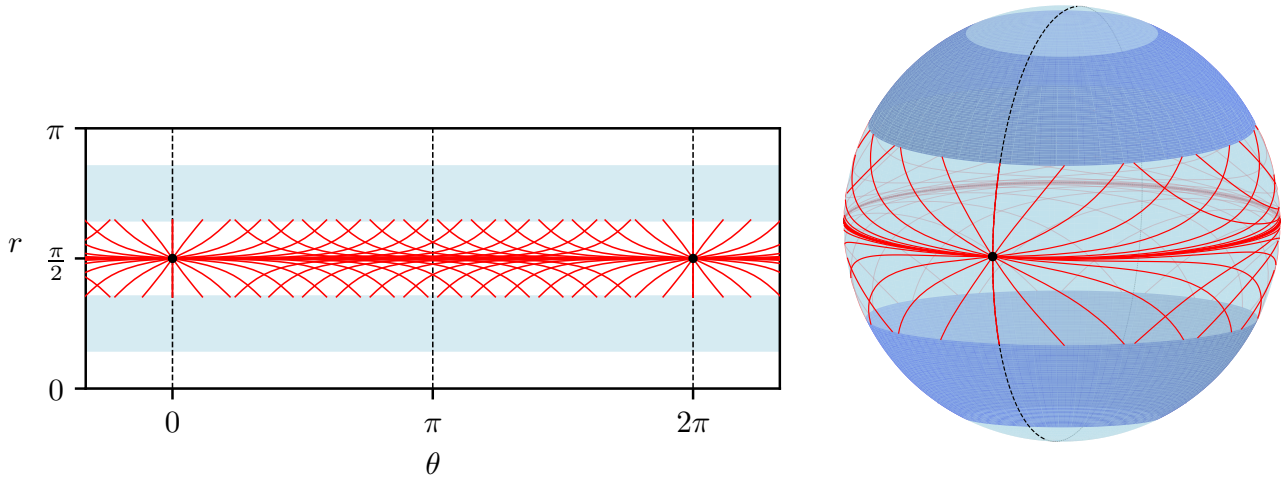

Figure 3: Lindblad problem: $\delta = 1.25$, $r_0 = \pi/2$. Geodesic flow. The red curves correspond to geodesics. The blue strips correspond to the domain of strong current.

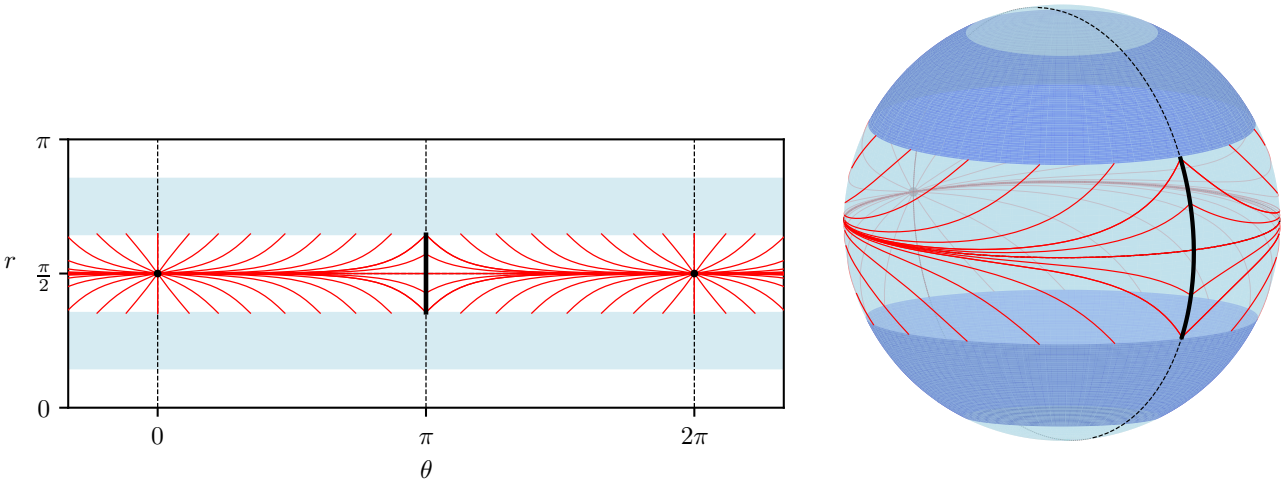

Figure 4: Lindblad problem: $\delta = 1.25$, $r_0 = \pi/2$. Synthesis. The red curves correspond to geodesics. The thick plain black line on the initial meridian is the cut locus. The blue strips correspond to the domain of strong current.

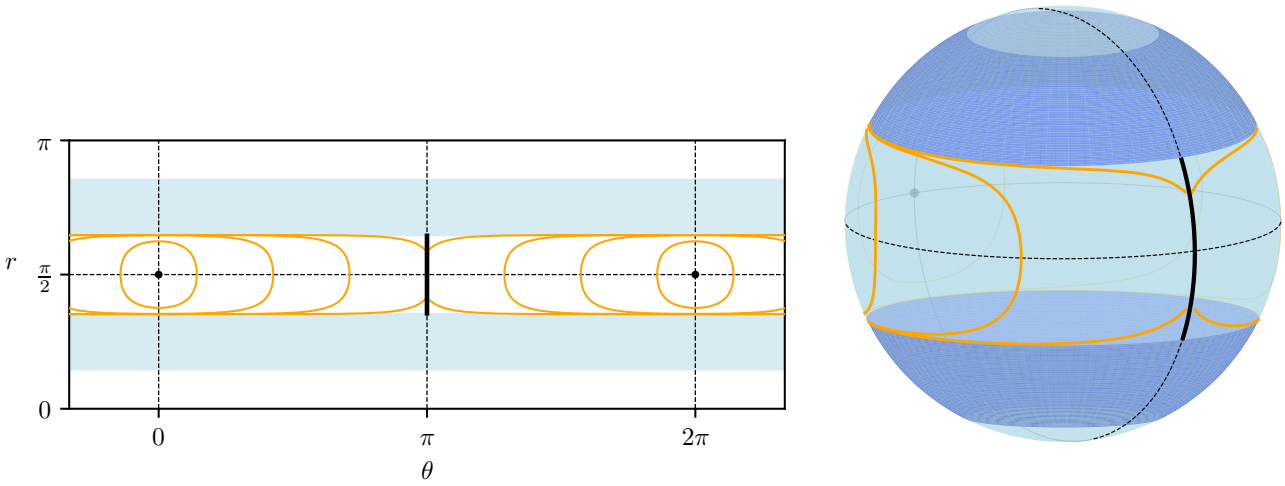

Figure 5: Lindblad problem: $\delta = 1.25$, $r_0 = \pi/2$. Spheres. The orange curves correspond to the spheres at times $t = \{1.0, 3.0, 5.0, 7.2\}$. The thick plain black line on the initial meridian is the cut locus. The blue strips correspond to the domain of strong current.

To complete the numerical simulations for the Lindblad problem, we provide geodesic flows in other settings, see Figures 6 and 7. In Figure 6, $\delta = -1.25$ and $r_0 = \pi/2$. This figure can be compared to Figure 3. We have represented only the right part of the geodesic flow, that is associated to $p_\theta \geq 0$. When δ is negative, the current is pointing up is the North hemisphere and down in the South one, which explains why the geodesics reach the regions of weak current around the poles. Once the geodesics are in these two regions, they are trapped due to the fact that the current has only a vertical component. The cut locus is more difficult to obtain in this case than for the case where $\delta = 1.25$ because of the folding of the geodesic flow inside the regions of weak current around the poles. In Figure 7, on the top, δ is positive while on the sub-figures at the bottom, δ is negative. One the left sub-figures, the initial point is in a region of strong current while for the right sub-figures, the initial point is in a region of weak current around the North pole. We can notice that when δ is positive, then the (hyperbolic) geodesics reach the region of weak current around the equator and then are trapped, converging to a barrier either in the North hemisphere or the South. When δ is negative the (hyperbolic) geodesics reach a region of weak current around the pole and then are trapped converging again to a barrier.

3.2 The averaged Kepler case

The Riemannian problem related to the averaged Kepler problem in space mechanics (see [3]) can be extended to a metric on a two-sphere of revolution defined in normal coordinates by

$$m^2(r) = \frac{\sin^2 r}{1 - \lambda \sin^2 r}$$

where λ is a homotopic parameter, deforming the round sphere (for $\lambda = 0$) to the singular metric called the *Grushin case* (for $\lambda = 1$) and $\lambda = 4/5$ corresponds to the *averaged Kepler case*. For this case, we will

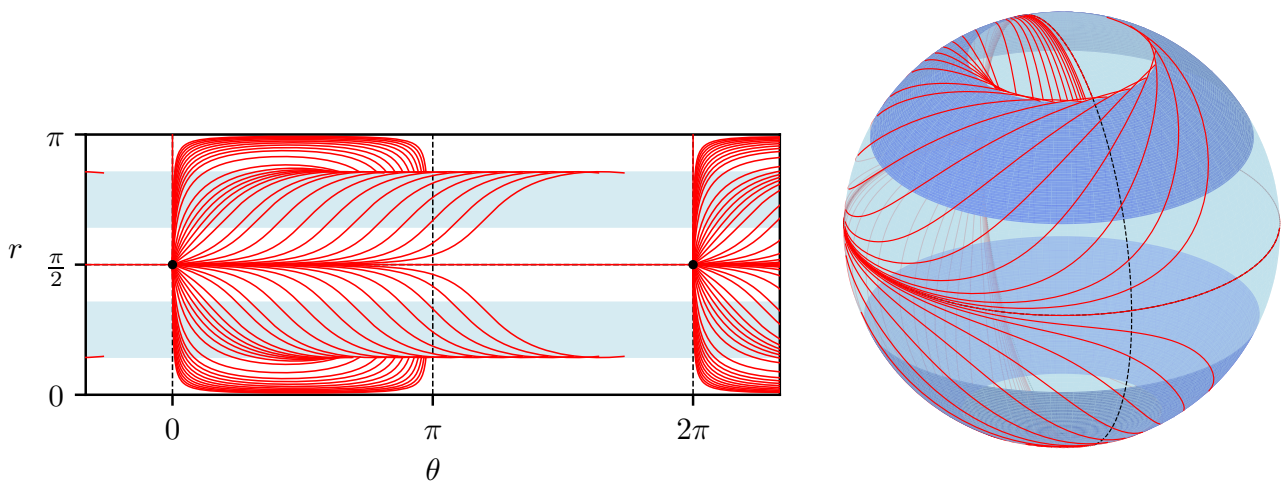

Figure 6: Lindblad problem: $\delta = -1.25$, $r_0 = \pi/2$. Geodesic flow. The red curves correspond to geodesics. The blue strips correspond to the domain of strong current.

consider a constant current on the covering space. The problem is thus given by

$$F_0 = v\frac{\partial}{\partial\theta}, \quad g = \mathrm{d}r^2 + m^2(r)\mathrm{d}\theta^2,$$

where v is a non-zero constant. Depending on the current at the initial point $q_0 = (r_0, \theta_0)$, we are in the weak (current) case if $\sin^2 r_0 < \frac{1}{v^2+\lambda}$, strong case if $\sin^2 r_0 > \frac{1}{v^2+\lambda}$ and moderate case if $\sin^2 r_0 = \frac{1}{v^2+\lambda}$. In the case where $v^2 + \lambda < 1$, the current will be weak on the whole domain. So we shall assume: $v^2 + \lambda > 1$. The following is a crucial geometric property.

Proposition 10. *On the two-sphere of revolution embedded in $\mathbb{R}^3$, the vector field F_0 defines a linear vector field, tangent to the sphere, and it corresponds to a uniform rotation whose axis is the axis of revolution. For the metric the equator solution is also a stationary rotation since $\frac{\mathrm{d}\theta}{\mathrm{d}t}$ is constant so that the effect of the current can be added to this rotation.*

Integration of the geodesics. From the previous proposition, the integration follows from the Riemannian case. Introducing the generalized potential, recall that the r-dynamics is given by:

$$\left(\frac{\mathrm{d}r}{\mathrm{d}t}\right)^2 = 1 - V(r, p_\theta).$$

Taking the ascending branch starting from the equator $r_0 = \pi/2$, we have

$$\frac{\mathrm{d}r}{\mathrm{d}t} = \left(\frac{p_\theta^2\,(1 - \lambda\sin^2 r)}{\sin^2 r\,(p^0 + p_\theta v)^2}\right)^{1/2},$$

Since $M = 0$, $\|p\|_g = -(p_\theta v + p^0)$, then, using a time reparameterization, one gets:

$$\frac{\mathrm{d}r}{\mathrm{d}s} = \left(\frac{p_\theta^2\,(1 - \lambda\sin^2 r)}{\sin^2 r}\right)^{1/2},$$

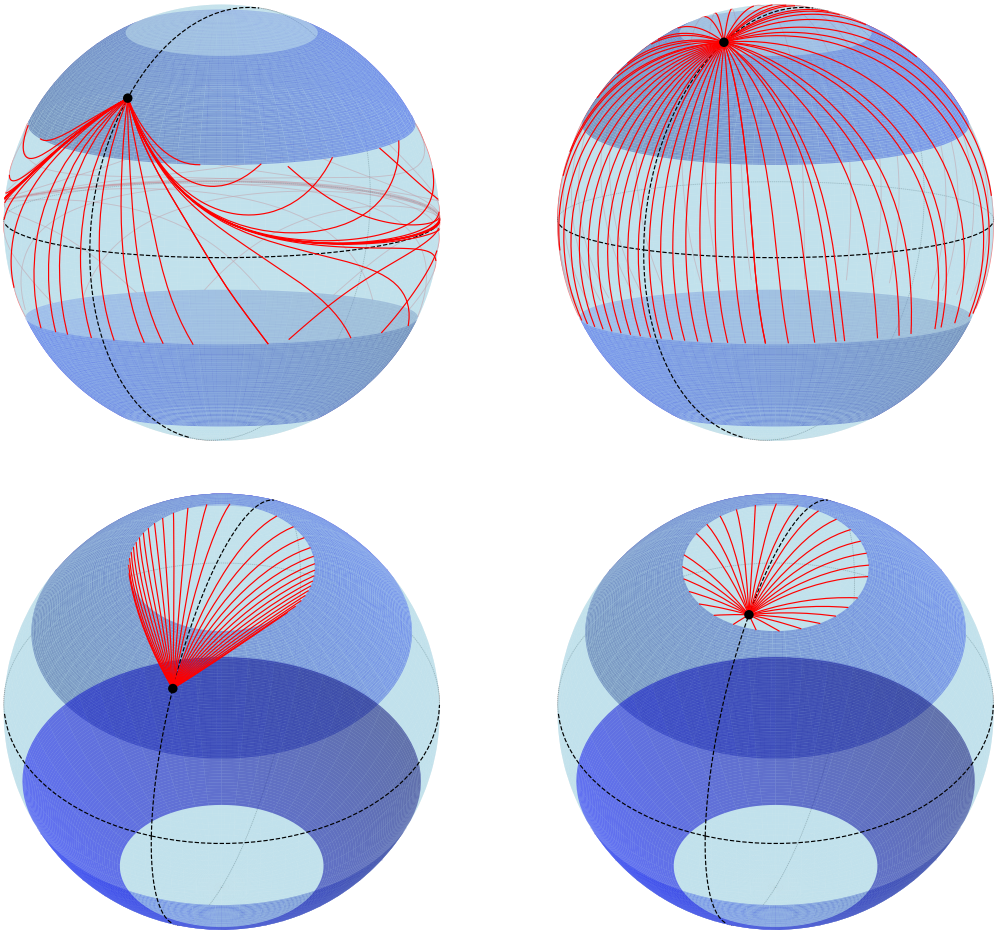

Figure 7: Lindblad problem: $\delta = 1.25$ (Top) and $\delta = -1.25$ (Bottom), $r_0 = \pi/2 + \pi/4$ (Left: strong current at r_0) and $r_0 = \pi/2 + 3\pi/8$ (Right: weak current at r_0). Geodesic flow. The red curves correspond to (hyperbolic) geodesics. The blue strips correspond to the domain of strong current.

which is like the r-dynamics in the Riemannian case, with the addition of v. Then, we can determine the first return mapping to the equator $r_0 = \pi/2$:

$$\frac{\Delta\theta}{2} = \int_{\pi/2}^{r_+} \frac{\partial M/\partial p_\theta}{\partial M/\partial p_r} \mathrm{d}r$$

where r_+ is the maximum of $r(t)$. See Figure 8 for an illustration of the geodesic flow.

The geodesic curves are symmetric with respect to the equator, the cone of admissible direction being symmetric with respect to the equator. This leads to the following stratification of the set of geodesics, using the variable p_θ.

Proposition 11. *Assume that $\lambda = 4/5$ and $v = 0.8$, then starting from the equator and considering only the ascending branch, geodesics split into (see also Figure 9):*

- *Abnormal given by $p_\theta^a = -1/v$;*

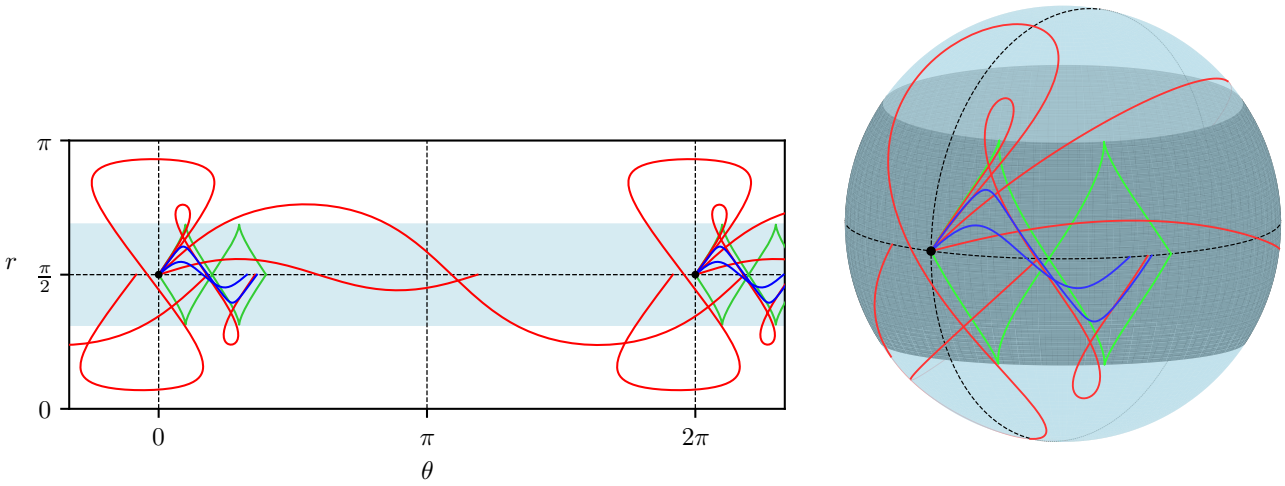

Figure 8: Kepler problem: $\lambda = 4/5$ and $v = 0.8$. Geodesic flow. The red curves correspond to hyperbolic geodesics. The green curves to abnormal and the blue curves to elliptic geodesics. The blue strip corresponds to the domain of strong current.

- *Hyperbolic geodesics parameterized by* $p_\theta \in (p_\theta^a, m(r_0))$*;*
- *Elliptic geodesics parameterized by* $p_\theta \in (-m(r_0), p_\theta^a)$*.*

Moreover, in the hyperbolic case, the set of geodesics can be stratified in four different classes:

- *The equator which corresponds to* $r = \pi/2$*,* $p_r = 0$ *and* $p_\theta = m(r_0)$*.*
- *The two pseudo-meridians (ascending and descending ones) which correspond, on the covering space, to the non-compact case where* $p_\theta = 0$*.*
- *Generic* r*-periodic orbits which split in two different families namely orbits without self-intersections, parameterized by* $p_\theta \in (0, m(r_0))$ *and orbits with self-intersections, parameterized by* $p_\theta \in (p_\theta^a, 0)$ *and* $\pm p_r(0)$ *corresponding to the symmetric orbits.*

Remark 2. The other geodesics in the flow are obtained by a symmetry with respect to the equator. See Figure 10 for the complete classification.

The cut locus in this case will split into two branches. See Figures 11 and 12 and 13. The first branch is associated to the cusp singularity of the abnormal directions, which are symmetric with respect to the equator. The second branch of the cut locus is the persistence of the segment formed by the equator and related to the tame behavior of the first return mapping corresponding to non self-intersecting geodesics. The conjugate points can be numerically evaluated. They exist for different types of geodesics but occur after the intersection of the geodesics with the equator.

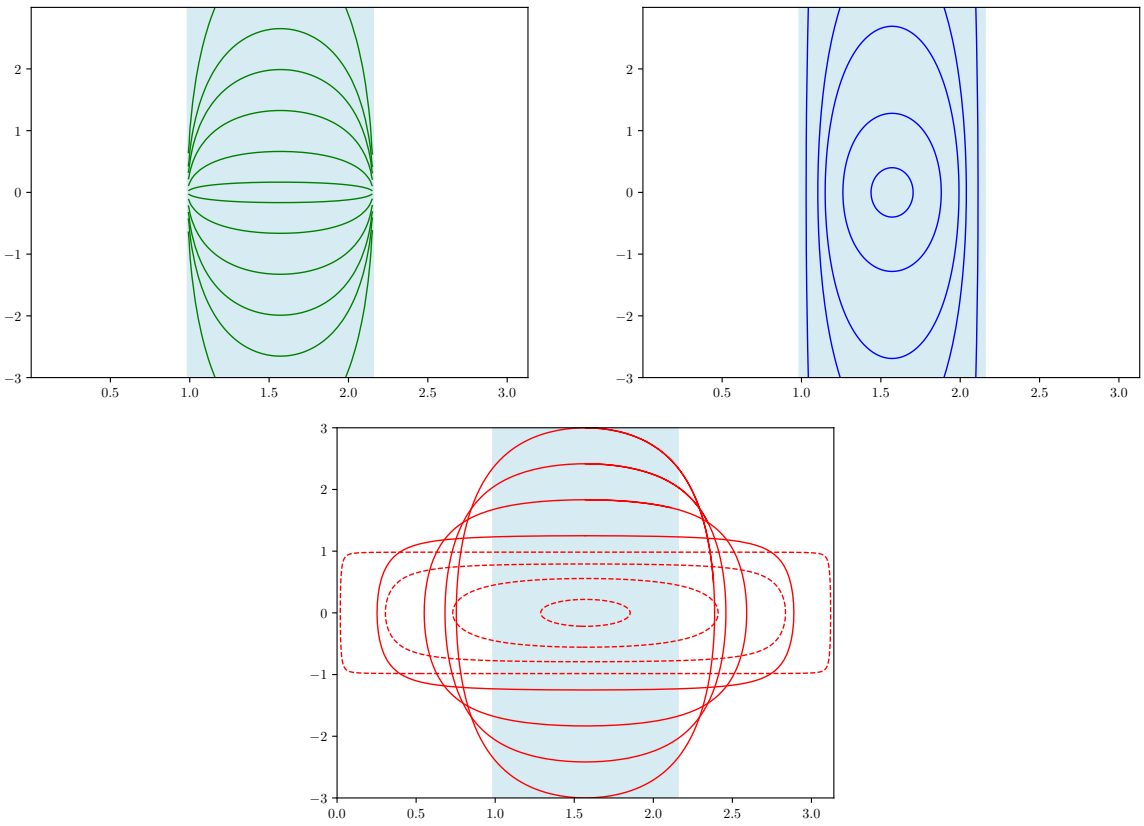

Figure 9: Kepler problem: $\lambda = 4/5$ and $v = 0.8$. Orbits in the (r, p_r) plane. The blue area represents the domain of strong current where the abnormal and elliptic extremals belong. Top-Left: abnormal orbits in green. Top-Right: elliptic orbits in blue. Bottom: hyperbolic orbits in red. The hyperbolic orbits without self-intersections are in dashed lines while orbits with self-intersections are in plain lines. The equator $r = \pi/2$ is a point at $(r, p_r) = (\pi/2, 0)$. The two pseudo-meridians give the transition between the two types of hyperbolic orbits. They correspond to the horizontal lines: $p_r = \pm 1$.

Theorem 5. *Assume that the equator $r_0 = \pi/2$ is in the strong current domain. Then the cut locus has two branches, the first branch being formed by the abnormal curves occurring in the neighborhood of the cusp point and associated to self-intersecting geodesics and the second branch being a segment of the equator, starting by a cusp point of the conjugate locus and associated to non self-intersecting geodesics.*

3.3 The Landau-Lifshitz model for ferromagnetic ellipsoidal samples

3.3.1 Model

This model is borrowed from [8]. We consider hereafter a particular Zermelo-type system modeling the behavior of magnetization in a ferromagnetic sample of ellipsoidal shape. We introduce the magnetization m and an external field u playing the role of a control, both being spatially uniform. Ellipsoidal domains have been much studied in the literature dedicated to ferromagnetism (see [12, 14, 18]).

According to [12, 14], for uniform (in space) magnetizations m on the ellipsoidal sample, the magnetization

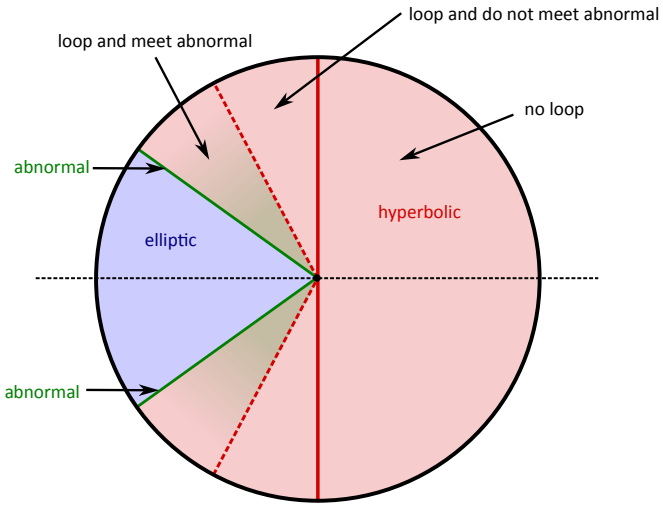

Figure 10: Kepler problem: $\lambda = 4/5$ and $v = 0.8$. Classification of the geodesics using the initial heading angle α_0 with the parameterization $p_\theta = m(r_0)\cos\alpha_0$ and $p_r(0) = \sin\alpha_0$. The term loop stands for self-interesting geodesics. The red vertical line separate the self-interesting hyperbolic geodesics to the hyperbolic geodesics without loops. The red dashed lines separate the hyperbolic geodesics interesting an abnormal to the one without intersection with any abnormal. The abnormals are represented by the green lines. The blue domain corresponds to the elliptic geodesics.

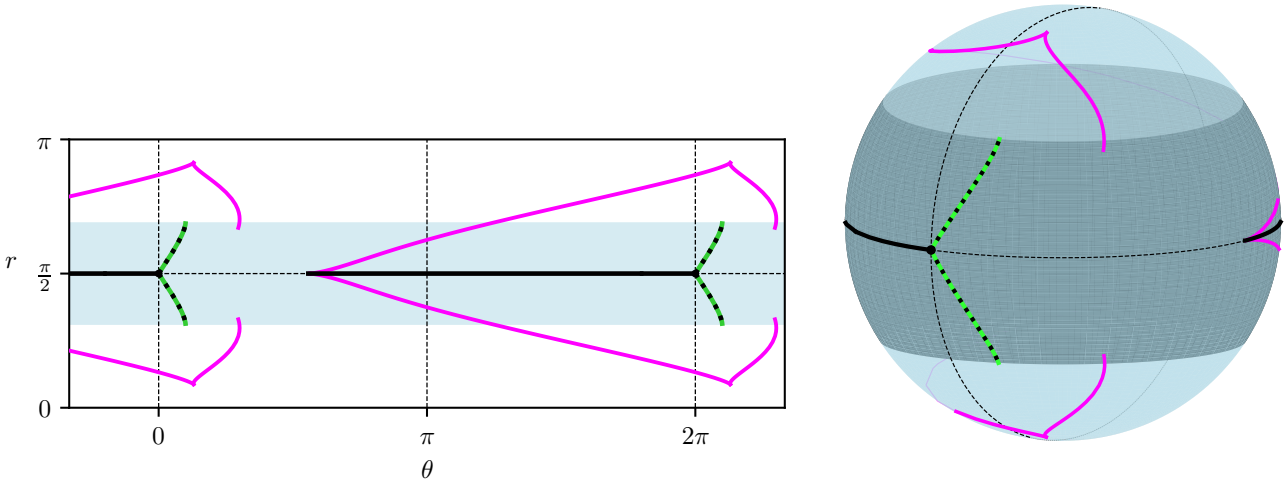

Figure 11: Kepler problem: $\lambda = 4/5$ and $v = 0.8$. Synthesis. The magenta curves correspond to the conjugate locus. The thick plain black line on the equator is one branch of the cut locus. The green curves are part of the two abnormals which are contained in the cut locus, that is why they are also represented by dashed black lines. The blue strip corresponds to the domain of strong current.

obeys the Landau-Lifshitz equation

$$\begin{cases} \dfrac{\mathrm{d}m}{\mathrm{d}t} = \alpha\left(h_0(m) - (h_0(m)\cdot m)m\right) - m \wedge h_0(m) \quad \text{in } (0,T) \\ m(0) = m^0 \end{cases} \tag{20}$$

where $\alpha > 0$ is a damping parameter, $h_0(m) = -Dm + u$ with a time-dependent external magnetic field

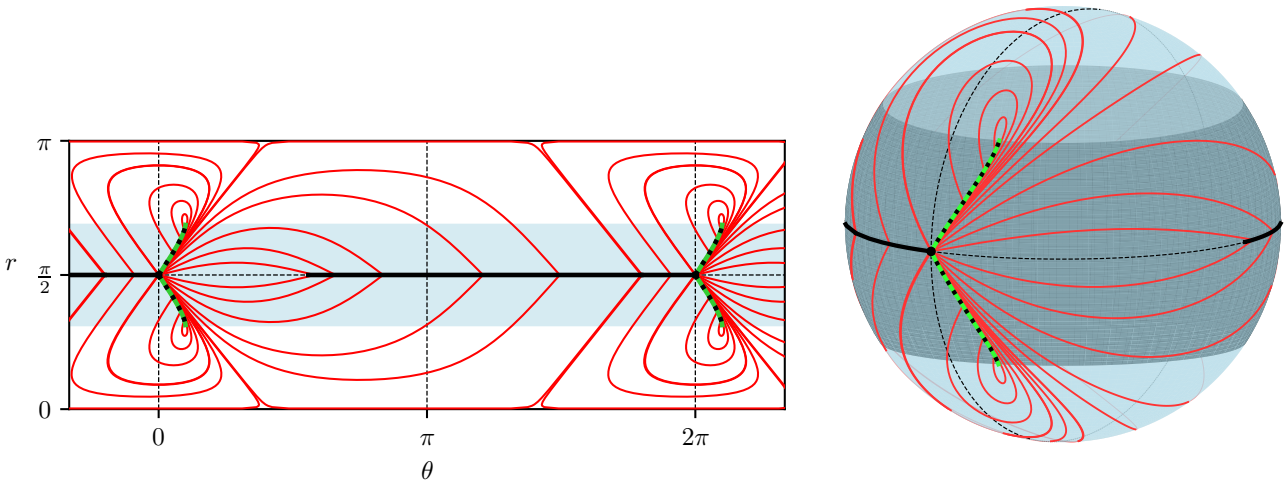

Figure 12: Kepler problem: $\lambda = 4/5$ and $v = 0.8$. Synthesis. The thick plain black line on the equator is one branch of the cut locus. The green curves are part of the two abnormals which are contained in the cut locus, that is why they are also represented by dashed black lines. The red curves correspond to hyperbolic geodesics until their cut points. The blue strip corresponds to the domain of strong current.

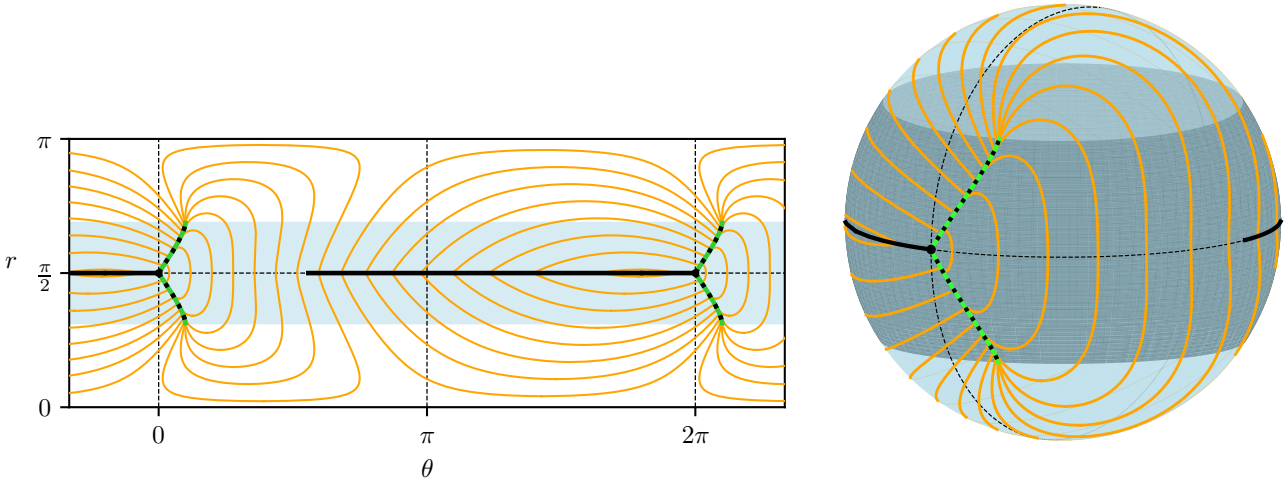

Figure 13: Kepler problem: $\lambda = 4/5$ and $v = 0.8$. Spheres. The orange curves correspond to spheres. One can notice the fan shape of spheres of small radii. The thick plain black line on the initial meridian is the cut locus. The green curves are part of the two abnormals which are contained in the cut locus, that is why they are also represented by dashed black lines. The blue strips correspond to the domain of strong current.

u, $T > 0$, $m(t) \in \mathbb{S}^2 \subset \mathbb{R}^3$, $D = \mathrm{diag}(\gamma_1, \gamma_2, \gamma_3)$ denotes a diagonal matrix with nonnegative coefficients, where each γ_i $(i = 1, 2, 3)$ is a constant depending only on the semi-axes. We refer for instance to [11] for the dependence of these coefficients on the geometry. Making a change of basis, we assume without loss of generality that $0 \leqslant \gamma_1 \leqslant \gamma_2 \leqslant \gamma_3 \leqslant 1$.

3.3.2 Reduction to a 2-sphere Zermelo problem

The control applied to the ferromagnetic sample is a control whose maximal intensity $U > 0$ is prescribed, which leads us to write

$$u = \begin{pmatrix} u_1 \\ u_2 \\ u_3 \end{pmatrix} \qquad u_1^2 + u_2^2 + u_3^2 \leqslant U^2 \quad \text{a.e. in } \mathbb{R}_+.$$

Using adequate changes of unknowns and time reparametrization[1], this leads to a control system of the form

$$\dot{q} = F_0(q) + \sum_{i=1}^{3} v_i F_i(q) \tag{21}$$

with $\|v\| \leqslant 1$.

Since the system evolves on the sphere, we introduce the coordinates

$$m = \begin{pmatrix} \cos r \\ \sin r \cos\theta \\ \sin r \sin\theta \end{pmatrix},$$

and we denote by $q = (r, \theta)$ the polar coordinates on the 2-sphere. Hence, the vector fields in (21) are given by

$$F_0(q) = \begin{pmatrix} \alpha\gamma_1 \cos r \sin r + (\gamma_2 - \gamma_3)\cos\theta \sin\theta \sin r - \\ \qquad\qquad \alpha(\gamma_2 \cos^2\theta + \gamma_3 \sin^2\theta)\cos r \sin r \\ \alpha(\gamma_2 - \gamma_3)\cos\theta\sin\theta - \gamma_1 \cos r + (\gamma_3 \sin^2\theta + \gamma_2 \cos^2\theta)\cos r \end{pmatrix},$$

$$F_1(q) = \begin{pmatrix} -\alpha \sin r \\ 1 \end{pmatrix}, \qquad F_2(q) = \begin{pmatrix} -\sin\theta + \alpha\cos\theta\cos r \\ -\dfrac{\alpha\sin\theta + \cos\theta\cos r}{\sin r} \end{pmatrix},$$

$$F_3(q) = \begin{pmatrix} \cos\theta + \alpha\sin\theta\cos r \\ \dfrac{\alpha\cos\theta - \sin\theta\cos r}{\sin r} \end{pmatrix}.$$

Proposition 12. *The Zermelo navigation problem associated to the Landau-Lifshitz model described above is associated to the maximized Hamiltonian*

$$M = \langle p, F_0(q)\rangle + \sqrt{p_r^2 + \frac{p_\theta^2}{\sin^2 r}} + p^0$$

where the parameters are such that $0 \leqslant \gamma_1 \leqslant \gamma_2 \leqslant \gamma_3$ and the metric is the standard metric on S^2 given by $g = dr^2 + \sin^2 r d\theta^2$ with constant curvature 1.

Proof. Let us denote by $G(q) = (F_1(q), F_2(q), F_3(q))$ the 2×3 matrix formed by concatenating the three vector fields. Denoting

$$e_1 = \begin{pmatrix} \frac{1}{\tan r} \\ \cos\theta \\ \sin\theta \end{pmatrix}, \qquad e_2 = \begin{pmatrix} 0 \\ -\sin\theta \\ \cos\theta \end{pmatrix} \qquad e_3 = \begin{pmatrix} \tan r \\ -\cos\theta \\ -\sin\theta \end{pmatrix},$$

[1]Namely, we consider the new control function $v(\cdot) = u(\cdot)/U$ and operate, with a slight abuse of notation, the change of variable $t \leftarrow t/U$. Moreover, we still denote by γ_i the real numbers γ_i/U.

one has

$$\operatorname{Ker} G(q) = \mathbb{R}e_1 \quad \text{and} \quad (\operatorname{Ker} G(q))^{\perp} = \operatorname{Span}\{e_2, e_3\}.$$

The basis (e_1, e_2, e_3) is orthonormal and direct, and moreover

$$\|e_3\|^2 = 1 + \tan^2 r = \frac{1}{\cos^2 r}.$$

Let us write the control v as

$$v = w_1 \frac{e_1}{\|e_1\|} + w_2 \frac{e_2}{\|e_2\|} + w_3 \frac{e_3}{\|e_3\|}$$

so that

$$Gv = w_2 \frac{Ge_2}{\|e_2\|} + w_3 \frac{Ge_3}{\|e_3\|} = w_2 \begin{pmatrix} 1 \\ \frac{\alpha}{\sin r} \end{pmatrix} + w_3 \begin{pmatrix} -\alpha \frac{|\cos r|}{\cos r} \\ \frac{|\cos r|}{\sin r \cos r} \end{pmatrix}.$$

One can assume by symmetry that q belongs to the Northern hemisphere so that $r \in [0, \pi/2]$, where $r = 0$ is the pole. Hence, we have

$$Gv \quad = \quad w_2 \begin{pmatrix} 1 \\ \frac{\alpha}{\sin r} \end{pmatrix} + w_3 \begin{pmatrix} -\alpha \\ \frac{1}{\sin r} \end{pmatrix}.$$

Hence, the controlled system rewrites as

$$\dot{q} = F_0(q) + G'w \quad \text{with} \quad G' = \begin{pmatrix} 1 & -\alpha \\ \frac{\alpha}{\sin r} & \frac{1}{\sin r} \end{pmatrix} = (G'_1, G'_2).$$

One has

$$\begin{aligned} \langle p, G'_1 \rangle^2 + \langle p, G'_2 \rangle^2 &= \left(p_r + \frac{\alpha}{\sin r} p_\theta \right)^2 + \left(-\alpha p_r + \frac{p_\theta}{\sin r} \right)^2 \\ &= (1 + \alpha^2) \left(p_r^2 + \frac{p_\theta^2}{\sin^2 r} \right). \end{aligned}$$

Hence, the maximized Hamiltonian reads

$$M = p.F_0(q) + \sqrt{1 + \alpha^2} \sqrt{p_r^2 + \frac{p_\theta^2}{\sin^2 r}} + p^0$$

and performing one more renormalization of the parameters γ_i, the proposition is proved. □

The dynamics of the Landau-Lifshitz system (20) reveal a certain richness when the parameters γ_i and α are varied, as illustrated by a wide variety of trajectory behaviours, see Figure 14. In particular, in [11], the existence of basins on the 2-sphere, from which trajectories cannot escape, thus acting as barriers, was demonstrated when the parameter α is chosen above a certain threshold. This phenomenon is illustrated in Figure 15, and reflects an obstruction to global controllability.

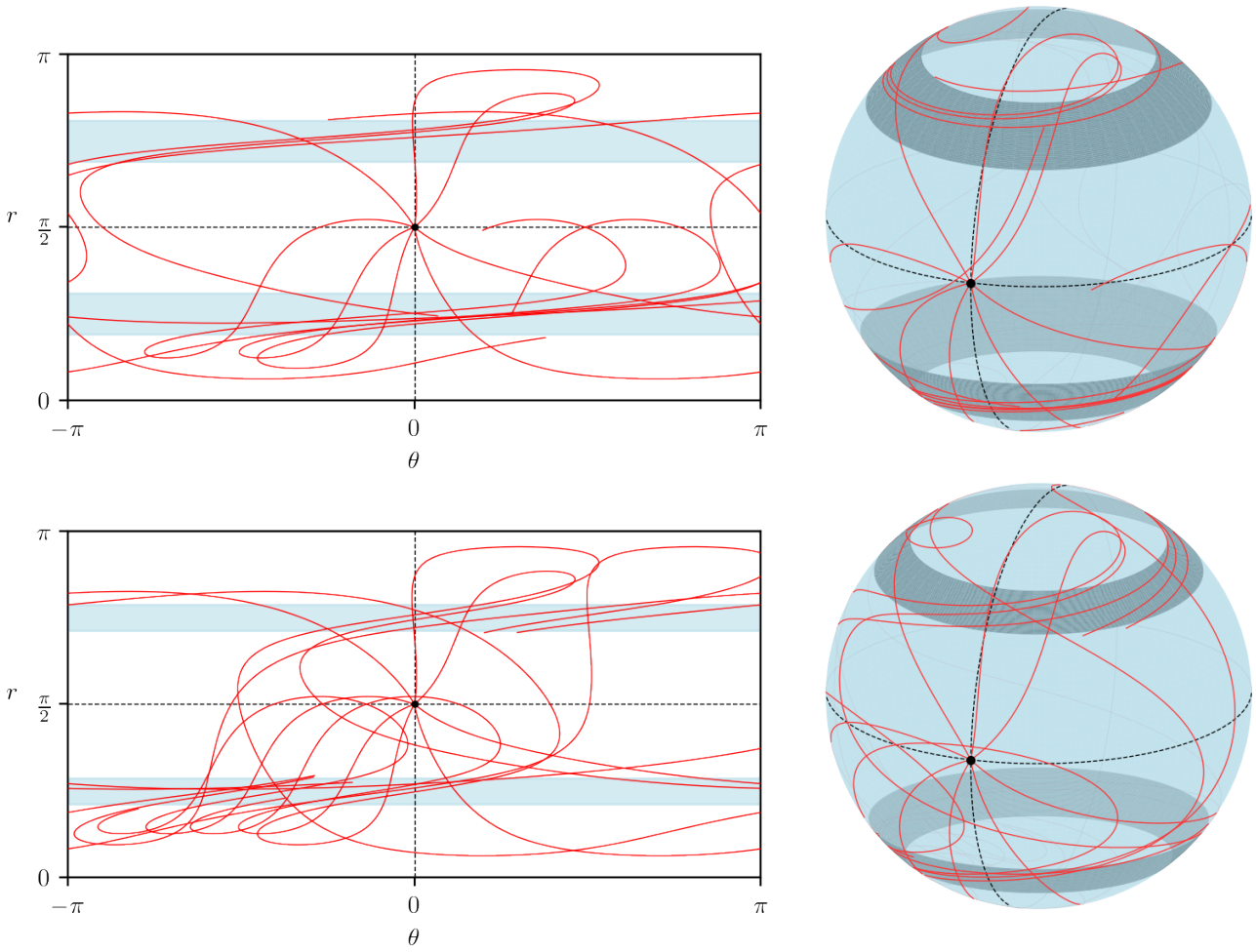

Figure 14: Case of revolution: $\alpha = 1.9$, $\gamma_2 - \gamma_1 = 1$. Example of trajectories. There are no confinement regions here.

3.3.3 Geometric properties and computation of $\|F_0\|_g = 1$

Let us use the notation

$$F_0(q) = \mu_1(q)\frac{\partial}{\partial r} + \mu_2(q)\frac{\partial}{\partial \theta}.$$

Proposition 13. *The domains corresponding to $\|F_0\|_g = 1$ are given by $\mu_1(g)^2 + \sin^2 r\,\mu_2(g)^2 = 1$, that is,*

$$(\alpha^2+1)\sin^2 r\left((\gamma_2-\gamma_3)^2\cos^2\theta\sin^2\theta + \cos^2 r\big(\gamma_1-\gamma_3-(\gamma_2-\gamma_3)\cos^2\theta\big)^2\right) = 1.$$

The case of revolution corresponds to $\gamma_2 = \gamma_3$.

The following proposition characterizes the existence of boundaries delimiting strong and weak currents zones (see Fig. 16). This comes to investigate the existence of solutions for the equation $\|F_0\|_g = 1$.

Proposition 14.

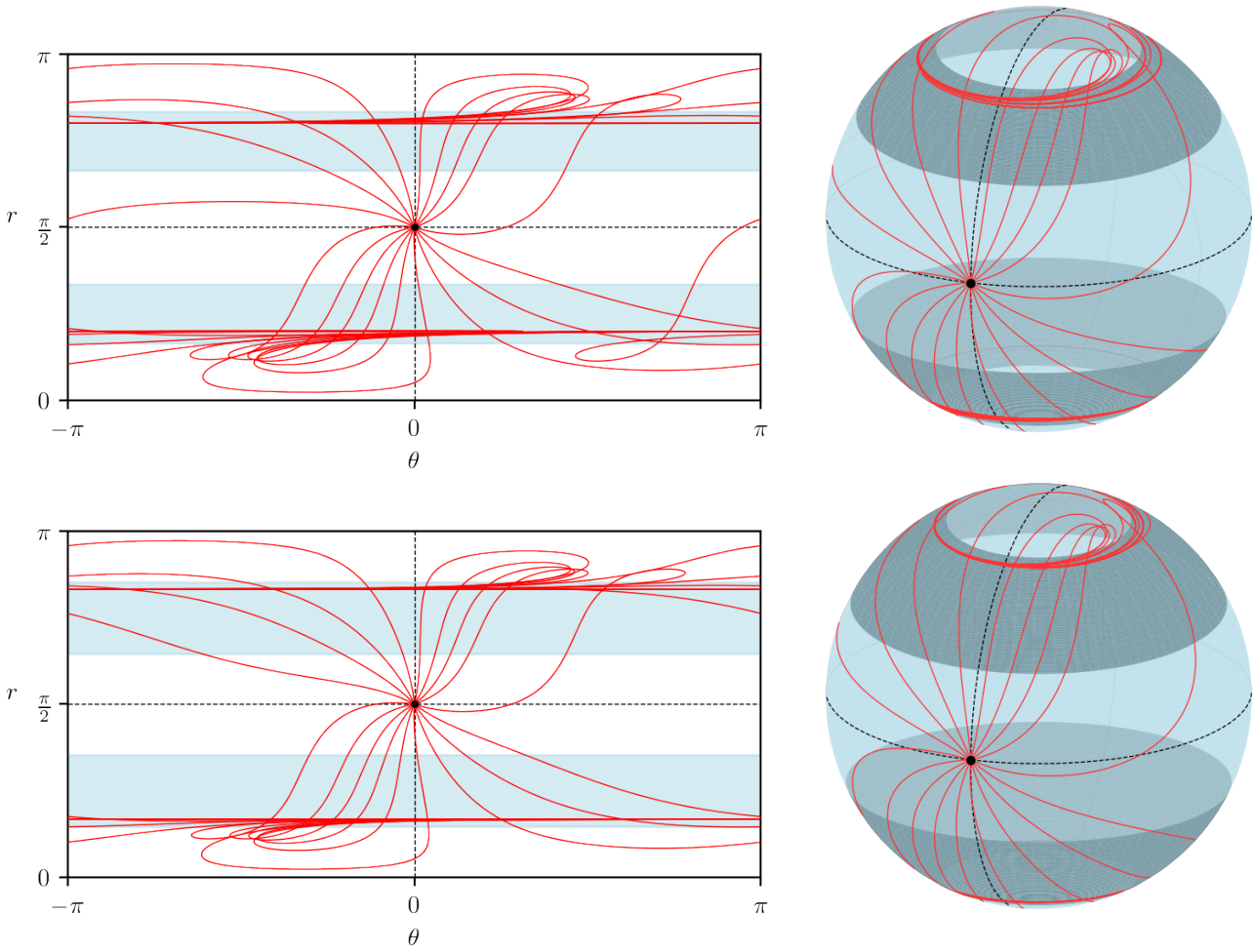

Figure 15: Case of revolution: $\alpha = 2.1$, $\gamma_2 - \gamma_1 = 1$. Example of optimal trajectories, illustrating the confinement regions from which the dynamics cannot escape.

1. *When $\gamma_2 < \gamma_3$, then a solution exists if the renormalized coefficients satisfy*

$$\frac{4}{(\alpha^2+1)(\gamma_1-\gamma_3)^2} \leqslant 1.$$

2. *In the case of revolution $\gamma_2 = \gamma_3$:*

   (a) *$\|F_0\|_g = 1$ is equivalent to*

$$1 = (\alpha^2+1)(\gamma_1-\gamma_3)^2 \sin^2 r \cos^2 r.$$

   (b) *A solution exists if and only if the renormalized coefficients satisfy*

$$\frac{4}{(\alpha^2+1)(\gamma_1-\gamma_3)^2} \leqslant 1.$$

Proof. We focus on the first point, the second being an easy consequence of the writing of the equation in the particular case $\gamma_2 = \gamma_3$. Hence, let us assume from now on that $\gamma_2 < \gamma_3$. For all $(i,j) \in \{1,2,3\}$, let us

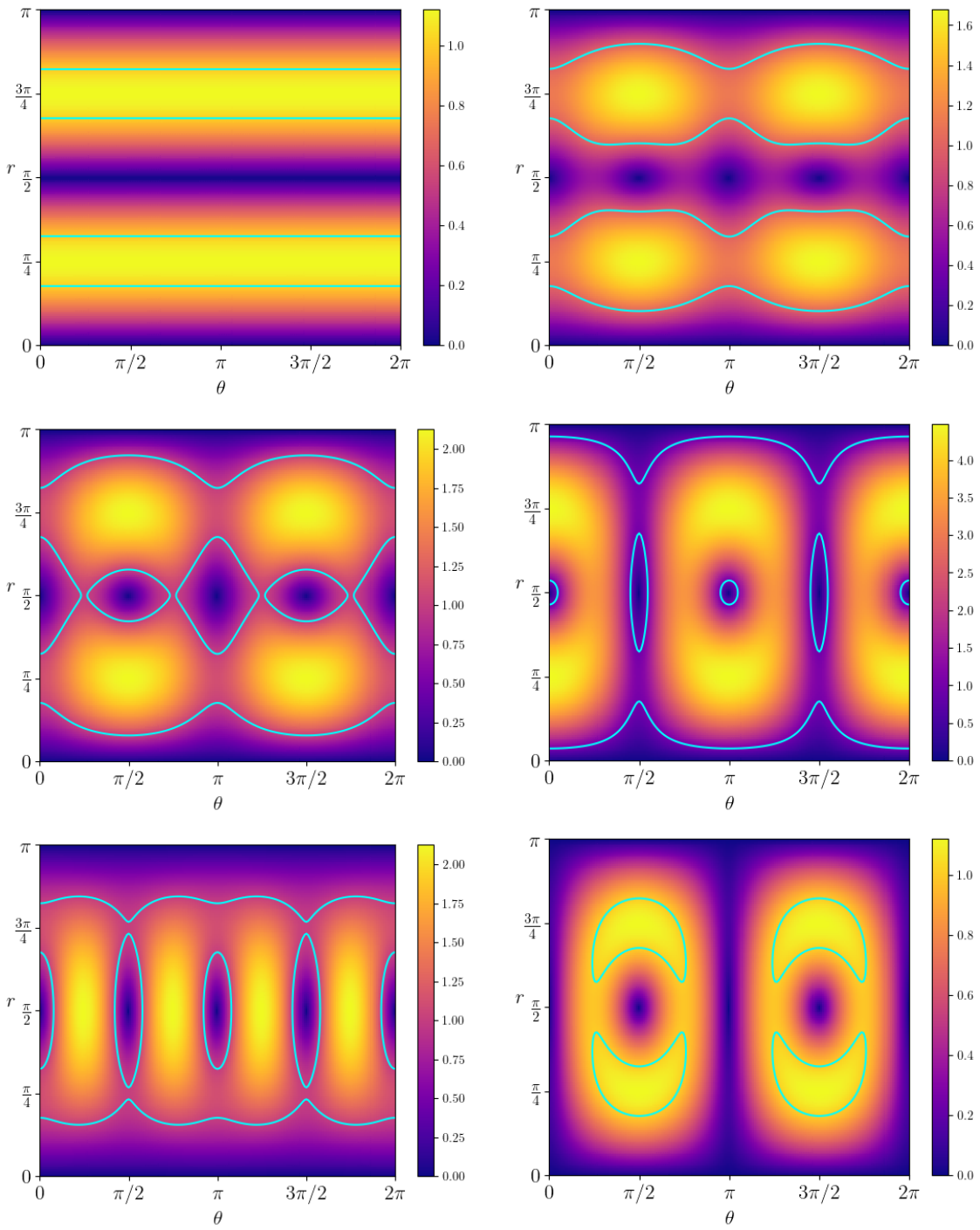

Figure 16: Boundary of weak and strong current domains on the 2-sphere. Top left: $\alpha = 2$, $\gamma_1 = 1$, $\gamma_2 = 2$, $\gamma_3 = 2$. Top right: $\alpha = 1$, $\gamma_1 = 2$, $\gamma_2 = 2.5$, $\gamma_3 = 2$. Middle left: $\alpha = 2$, $\gamma_1 = 1$, $\gamma_2 = 2$, $\gamma_3 = 2.9$. Middle right: $\alpha = 2$, $\gamma_1 = 1$, $\gamma_2 = 5$, $\gamma_3 = 2$. Bottom left: $\alpha = 2$, $\gamma_1 = 2.9$, $\gamma_2 = 3.9$, $\gamma_3 = 2$. Bottom right: $\alpha = 2$, $\gamma_1 = 2.9$, $\gamma_2 = 3.9$, $\gamma_3 = 2$.

set $\gamma_{ij} = \gamma_i - \gamma_j$, and $c = 1/(\alpha^2+1)$. It is straightforward to see that solving $\|F_0\|_g = 1$ is equivalent to the existence of a pair (r,θ) such that $\varphi_\theta(\sin r) = 0$, where

$$\begin{aligned}\varphi_\theta(X) &= (\gamma_{31} - \gamma_{32}\cos^2\theta)^2 X^2 - (\gamma_{32}^2\cos^2\theta\sin^2\theta + (\gamma_{31} - \gamma_{32}\cos^2\theta)^2)X + c\\ &= (\gamma_{31} - \gamma_{32}\cos^2\theta)^2 X^2 - (\gamma_{21}^2\cos^2\theta + \gamma_{31}^2\sin^2\theta)X + c.\end{aligned}$$

Hence, a solution exists if that there exists $\theta \in [0, 2\pi]$ such that the equation $\varphi_\theta(X) = 0$ has a solution in $[0,1]$.

Let us assume temporarily that $\gamma_{21} > 0$ so that the leading coefficient of the polynomial $\varphi_\theta(X)$ is non degenerated. One has

$$\varphi'_\theta(X) = 2(\gamma_{31} - \gamma_{32}\cos^2\theta)^2 X - (\gamma_{21}^2\cos^2\theta + \gamma_{31}^2\sin^2\theta)$$

and therefore, $\varphi'_\theta(0) = -(\gamma_{21}^2\cos^2\theta + \gamma_{31}^2\sin^2\theta) < 0$. The function φ_θ is then convex and decreasing in a neighborhood of 0. A solution thus exists provided that there exists $\theta \in [0, 2\pi]$ such that

$$\min_{X\in\mathbb{R}} \varphi_\theta(X) \leqslant 0 \quad \text{and} \quad \Big(\varphi'_\theta(1) \geqslant 0 \quad \text{or} \quad \varphi_\theta(1) \leqslant 0\Big).$$

We compute

$$\begin{aligned}\varphi'_\theta(1) &= 2\gamma_{32}^2\cos^4\theta - \gamma_{32}(\gamma_{32} + 2\gamma_{31})\cos^2\theta + \gamma_{31}^2\\ \varphi_\theta(1) &= c - \gamma_{32}^2\cos^2\theta\sin^2\theta\\ \min_{\mathbb{R}} \varphi_\theta &= c - \frac{(\gamma_{21}^2\cos^2\theta + \gamma_{31}^2\sin^2\theta)^2}{(\gamma_{21}\cos^2\theta + \gamma_{31}\sin^2\theta)^2}\end{aligned}$$

and we obtain the necessary existence condition by noting that

$$\max_{\mathbb{R}} \varphi'_0(1) = \gamma_{21}^2 > 0 \quad \text{and} \quad \min_{\mathbb{R}} \varphi_0 = c - \frac{\gamma_{31}^2}{4}.$$

Consider now the case $\gamma_{21} = 0$. The equation rewrites

$$\frac{1}{\gamma_{32}^2(\alpha^2+1)} = \sin^2 r\sin^2\theta(1 - \sin^2 r\sin^2\theta).$$

Since

$$\max_{r,\theta} \sin^2 r\sin^2\theta(1 - \sin^2 r\sin^2\theta) = 1/4,$$

the expected conclusion follows. □

4 Conclusion

In this article we have developed and applied some techniques of geometric optimal control to classify and analyze Zermelo navigation problems on two-spheres of revolution. We have illustrated our results on three case studies, in the fields of quantum control, of orbital transfer and of micromagnetism, providing some numerical simulations. Our findings can be used further to evaluate the fixed time accessibility sets and their boundaries, for instance by combining the techniques of the present paper with a NMPC method (see [17]).

References

[1] V. I. Arnold. *Mathematical methods of classical mechanics*, volume 60 of *Graduate Texts in Mathematics*. Springer-Verlag, New York, second edition, 1989. Translated from the Russian by K. Vogtmann and A. Weinstein.

[2] A. V. Bolsinov and A. T. Fomenko. *Integrable Hamiltonian systems*. Chapman & Hall/CRC, Boca Raton, FL, 2004. Geometry, topology, classification, Translated from the 1999 Russian original.

[3] B. Bonnard and J.-B. Caillau. Geodesic flow of the averaged controlled Kepler equation. *Forum Math.*, 21(5):797–814, 2009.

[4] B. Bonnard and M. Chyba. *Singular trajectories and their role in control theory*, volume 40 of *Mathématiques & Applications (Berlin) [Mathematics & Applications]*. Springer-Verlag, Berlin, 2003.

[5] B. Bonnard, O. Cots and B. Wembe. Zermelo navigation problems on surfaces of revolution and geometric optimal control. *ESAIM: Control, Optimisation and Calculus of Variations*, 29:60, 2023.

[6] B. Bonnard, J. Rouot and B. Wembe. Accessibility properties of abnormal geodesics in optimal control illustrated by two case studies. *Mathematical Control and Related Fields*, 13(4):1618–1638, 2023.

[7] B. Bonnard and D. Sugny, *Time-minimal control of dissipative two-level quantum systems: The integrable case*, SIAM J. Control Optim., **48** (2009), no. 3, 1289–1308.

[8] W. F. Brown, *Micromagnetics*, Interscience publishers, 1963, New York.

[9] A. E. Bryson. *Applied optimal control: optimization, estimation and control*. Routledge, 2018.

[10] C. Carathéodory. *Calculus of variations and partial differential equations of the first order. Part II: Calculus of variations*. Holden-Day, Inc., San Francisco, Calif.-London-Amsterdam, 1967. Translated from the German by Robert B. Dean, Julius J. Brandstatter, translating editor.

[11] R. Côte, C. Courtès, G. Ferrière and Y. Privat. Minimal time of magnetization switching in small ferromagnetic ellipsoidal samples. *arXiv preprint arXiv:2301.03839*, 2023.

[12] G. Di Fratta. The newtonian potential and the demagnetizing factors of the general ellipsoid. *Proceedings of the Royal Society A: Mathematical, Physical and Engineering Sciences*, 472(2190):20160197, 2016.

[13] K. R. Meyer and G. R. Hall. *Introduction to Hamiltonian dynamical systems and the N-body problem*, volume 90 of *Applied Mathematical Sciences*. Springer-Verlag, New York, 1992.

[14] J. A. Osborn. Demagnetizing factors of the general ellipsoid. *Physical review*, 67(11–12):351, 1945.

[15] A. Pelayo and S. Vu Ngoc. Symplectic theory of completely integrable hamiltonian systems. *Bulletin of the American Mathematical Society*, 48(3):409–455, 2011.

[16] L. S. Pontryagin, V. G. Boltyanskii, R. V. Gamkrelidze, and E. F. Mishchenko. *The mathematical theory of optimal processes*. Interscience Publishers John Wiley & Sons, Inc., New York-London, 1962. Translated from the Russian by K. N. Trirogoff; edited by L. W. Neustadt.

[17] J. B. Rawlings, D. Q. Mayne and M. Diehl, *Model predictive control: theory, computation, and design*, Vol. 2. Madison, WI: Nob Hill Publishing, 2017.

[18] D. Takahashi and V. C. Oliveira Jr. Ellipsoids (v1. 0): 3-D magnetic modelling of ellipsoidal bodies. *Geoscientific Model Development*, 10(9):3591–3608, 2017.

[19] R. J. Walker. *Algebraic curves*, volume 58. Springer, 1950.

[20] J. Williamson. *On the algebraic problem concerning normal forms of linear dynamical systems*. Amer. J. Math. 58 (1936) 141–163. 42.

[21] E. Zermelo. Über das navigationsproblem bei ruhender oder veränderlicher windverteilung. *ZAMM-Journal of Applied Mathematics and Mechanics/Zeitschrift für Angewandte Mathematik und Mechanik*, 11(2):114–124, 1931.